Nonlinear Dyn (2021) 106:681–706
https://doi.org/10.1007/s11071-021-06682-y

ORIGINAL PAPER

Identification of time-varying nonlinear structural physical parameters by integrated WMA and UKF/UKF-UI

Ning Yang · Jun Li · Ying Lei · Hong Hao

Received: 15 November 2020 / Accepted: 23 June 2021 / Published online: 27 August 2021

Abstract The identification of time-varying physical parameters of nonlinear systems is still a challenging task. Limited studies based on the wavelet multiresolution analysis (WMA) have been attempted, which requires full measurements of structural displacement, velocity and acceleration responses of all degrees of freedom and exact information of external excitations. This limits the engineering application of these methods. This paper proposes approaches to identify the time-varying physical parameters of nonlinear structures in three cases using only partially measured structural responses. Firstly, the identification of time-varying nonlinear structures with a small number of elements under known excitations is discussed. The fading-factor unscented Kalman filter (FUKF) method is applied to locate the time-varying parameters, and the WMA integrated with UKF method is employed using partially measured acceleration responses. Secondly, it is further extended to the identification of time-varying nonlinear structures with a small number of elements but under unknown excitations. An improved fading-factor unscented Kalman filter under unknown input (FUKF-UI) method is proposed to locate the time-varying parameters, and WMA integrated with UKF-UI method is utilized with partially observed acceleration and displacement responses. Thirdly, for practical engineering applications, the identification of time-varying nonlinear structure with more elements under unknown excitations is conducted. The proposed FUKF-UI method is employed to locate the time-varying parameters of the whole structure. Then, the whole structure is divided into several substructures and the unknown interaction forces are regarded as the fictitious unknown inputs to the substructure. Thus, physical parameters of each substructure can be identified in parallel by the combination of WMA and UKF-UI. Three numerical studies corresponding to these three cases are conducted, respectively, to demonstrate the effectiveness and accuracy of the proposed methods.

Keywords Nonlinear time-varying structures · Wavelet multiresolution · Unscented Kalman filter · Unknown excitation · Incomplete measurements · Substructural method

N. Yang
Department of Instrumental and Electrical Engineering, Xiamen University, Xiamen, China

N. Yang · J. Li · H. Hao
Centre for Infrastructural Monitoring and Protection, School of Civil and Mechanical Engineering, Curtin University, Bentley, WA, Australia

Y. Lei (✉)
Department of Civil Engineering, Xiamen University, Xiamen, China
e-mail: ylei@xmu.edu.cn

1 Introduction

Time-varying properties are common for structures in service due to severe natural and manmade hazards, resulting in that the identification of time-varying structural systems is a very important research topic [1, 2]. Bao et al. [3] conducted a comprehensive state-of-the-art review of data science and engineering in structural health monitoring, accessed the conditions and identified the occurrence of damages using machine learning algorithms. The quasi-static monitoring data are rarely analyzed and utilized in damage detection, Bao and Li [4] performed pattern recognition on quasi-static monitoring data, and proposed approach through the variation of pattern parameters. The results are so promising that this study made the static monitoring data be useful and open a new field for structural health monitoring. Effective methods have been investigated to identify the time-varying physical parameters, such as the state space model-based methods [5–7] in the time domain, or the wavelet multiresolution analysis (WMA)-based methods [8–12] in the time–frequency domain. In particular, WMA has an excellent function on arbitrarily adjustable time–frequency resolution. Most existing WMA-based methods expand the time-varying structural physical parameters into scale coefficients and then identify these coefficients by the linear least-squares estimation [8–10]. However, it is required that the displacement, velocity, acceleration responses at all degrees of freedom (DOFs) and external load information are known in these methods, which is a tough condition in actual applications. To overcome the limitation on full observations, novel methods have been proposed [11, 12] recently by the authors to identify the time-varying linear structures under known or unknown excitations using partial measurements based on the synthesis of WMA and Kalman filter (KF), transforming the solution of scale coefficients into a nonlinear least-squares optimization problem. However, it is required to expand all physical parameters, including time-varying parameters and time-invariant parameters, into scale coefficients based on WMA. With the growing number of scale coefficients, the difficulty of least-squares optimization is heavily increased.

Moreover, these above-mentioned methods are proposed based on the assumption of the linear model. However, under strong external loads such as earthquake, strong wind, impact and explosion, engineering structural components may present nonlinear behavior intrinsically [13–15]. Xu et al. [14] successfully analyzed the nonlinear failure mechanism of reinforced concrete columns under earthquake based on a region-based deep convolutional neural network. In recent years, many scholars have carried out in-depth researches on the identification of nonlinear structural characteristics and presented a variety of identification methods, including time-domain [16–19], frequency-domain [20] or time–frequency analysis methods [21–27]. However, the parameters of nonlinear models are assumed to be steady in most of these methods, only a few efforts have been attempted on the identification of time-varying nonlinear systems. Adaptive identification techniques based on KF have the potential to track time-varying parameters of hysterically degrading structures [5–7], which exploited the track factor, adaptive correction factor or adaptive factor matrix to deal with the evolution of system variation. The challenging issue is that either these adaptive algorithms have strong subjectivity on empirical factors [7], or it is time-consuming in calculating the optimal matrix at each time step [6]. The WMA-based method mentioned above can also be used to identify the time-varying nonlinear systems. For instance, Chang and Shi [27] proposed a method to identify the time-varying physical parameters and model parameters in the Bouc–Wen hysteresis model based on WMA. However, this method needs full information on the structural displacement, velocity, acceleration responses and excitation. Furthermore, in addition to the stiffness and damping parameters, the parameters in the nonlinear model are also needed to be expanded by WMA, which increases the complexity than the identification of linear systems.

With partial measurements, the extended Kalman filter (EKF) and unscented Kalman filter (UKF) [28] have been commonly used in the identification of nonlinear time-invariant systems. Compared with EKF, UKF is more superior as it does not need the calculation of the Jacobian matrix and a linearization-based approximation of the nonlinear system, realizing an on-line identification with a better recognition accuracy [29]. Furthermore, the UKF method for the case of unknown excitations has been derived and successfully applied to the physical parameter identification of nonlinear systems under unknown loads [30]. However, these methods are only suitable for the

time-invariant systems. Adaptive UKF methods have been proposed for the identification of time-varying structures, combining with the adjustment of error covariance [31–33] or the adjustment of noise covariance matrix [34, 35]. This may depend on the fading factors in most of the developed methods. However, if the fading factors are not selected properly, one may only roughly judge which parameter has the most possibility of varying property, but the change degree is difficult to be accurately determined. Moreover, all these adaptive methods are derived on the premise of known excitation. To the best knowledge of the authors, there is a lack in the identification of time-varying nonlinear systems under unknown excitations.

In addition, it should be pointed out that the existing WMA-based methods are only applicable to structures with a small number of elements [8–12, 27]. The reason is that the number of scale coefficients in the least-squares process will increase with the number of elements, which makes it difficult to obtain the global optimal solution especially when the quality of observation data is poor. The "divide and conquer" idea of the substructural-based methods provides a feasible strategy for the identification of structures with more elements [36–40]. Many scholars have also introduced the concept of substructure into the identification of nonlinear structures [41–44]. However, these methods are mostly used to identify the parameters of time-invariant systems, and they still have some shortcomings such as the difficulties in determining the interface forces, the incapability of parallel identification and the existence of propagation errors [45]. Shi and Chang [46, 47] presented an offline substructural method to identify the time-varying nonlinear shear-type buildings based on WMA. Nevertheless, the method requires all the displacement, velocity and acceleration responses inside and at the interfaces of the substructure. Further development and studies on identification techniques for time-varying nonlinear structures with more elements are still needed.

Based on the above-mentioned detailed literature, most WMA-based methods are used to identify the physical parameters of time-varying linear systems, while only a few studies are conducted for the time-varying nonlinear systems. In addition, these methods require full measurements of displacement, velocity, acceleration and external loads. Furthermore, all physical parameters including time-varying and time-invariant parameters are expanded by WMA, which leads to a significant increase in the number of scale coefficients. Therefore, two-step identification processes are proposed in this paper to identify the physical parameters of time-varying nonlinear systems by using partial measurements. Three cases are discussed, respectively. The first case is the identification of time-varying nonlinear structures with a small number of elements under known excitations. The time-varying physical parameters are located by the fading-factor unscented Kalman filter (FUKF) in the first step, and the method integrating WMA with UKF is proposed to identify the time-varying physical parameters in the second step, which uses partially measured acceleration responses. A numerical example of a six-story time-varying nonlinear shear frame under known seismic acceleration is provided, with abruptly changed or gradually varying parameters, to verify the effectiveness of the first proposed identification process. Considering that the external loads are always hard to measure in practical situations, the study is extended to the second case, that is, the identification of time-varying nonlinear structures with a small number of elements but under unknown excitations. Herein, the improved unscented Kalman filter under unknown input (UKF-UI) method proposed by the authors [30] is adopted. The time-varying physical parameters are located by the proposed fading-factor UKF-UI (FUKF-UI) in the first step, and the method integrating WMA with UKF-UI is proposed to identify the physical parameters using partially measured acceleration and displacement responses in the second step. The numerical study on a truss structure is conducted to identify the time-varying parameters and unknown excitations simultaneously. The last case is the identification of time-varying nonlinear structures with more number of elements under unknown excitations, which is investigated based on the substructural method. The time-varying physical parameters of the whole structure are located by the proposed FUKF-UI method in the first step. In the second step, the whole structure is divided into several substructures and the unknown interaction force is considered as the fictitious "unknown input". Therefore, each substructure can be identified in parallel using the proposed WMA integrated with UKF-UI method. The numerical study on a ten-story shear frame demonstrates that the third proposed identification process is effective for the identification

of structures with more number of elements under unknown excitations.

The remaining part of this paper is organized as: Sect. 2 presents the identification process and numerical validation of time-varying nonlinear structures with a small number of elements under known excitations. Section 3 is extended to the case of time-varying nonlinear structures with a small number of elements but under unknown excitations. Section 4 further extends the study to the case of time-varying nonlinear structures with more number of elements under unknown excitations by using the substructural method. Finally, some conclusions with recommendations on the further research are presented in Sect. 5.

2 Identification of time-varying nonlinear structures with a small number of elements under known excitations

2.1 The proposed two-step identification process

The expansion of all physical parameters, including stiffness parameters, damping parameters and nonlinear model parameters, leads to a large number of scale coefficients. This increases the possibility of not obtaining local optimization solutions, especially for the case with poor-quality measurement data. Thus, it is difficult or even impossible to obtain global optimal scale coefficients when the number of unknown parameters is large. In fact, the time-varying physical parameters are always sparse in the systems [38]. The time-invariant parameter can be identified directly as a time-invariant coefficient. It is not necessary to expand all parameters into scale coefficients by WMA, which increases the number of coefficients to be identified for the time-invariant parameters instead. This paper proposes a two-step identification process for the time-varying nonlinear physical parameters. The time-varying parameters are localized using the FUKF method in the first step. Then an objective function is constructed based on WMA and UKF in the second step, which is the implicit function of the time-invariant physical parameters and scale coefficients of time-varying parameters. Finally, these unknown variables are solved by the nonlinear least-squares optimization. The detailed procedure is introduced as follows.

2.1.1 *Locate the time-varying physical parameters by the FUKF method*

The equation of motion of a time-varying nonlinear system is described as:

$$\mathbf{M}\ddot{\mathbf{x}}(t) + \mathbf{R}(\boldsymbol{\theta}(t), \mathbf{x}(t), \dot{\mathbf{x}}(t)) = \boldsymbol{\eta}\mathbf{f}(t) \tag{1}$$

in which $\mathbf{M}$ is the time-invariant and known mass matrix, $\mathbf{f}$ is the known excitation with the influence matrix $\boldsymbol{\eta}$, $\mathbf{x}$, $\dot{\mathbf{x}}$ and $\ddot{\mathbf{x}}$ are displacement, velocity and acceleration vector, respectively, $\boldsymbol{\theta}$ is the vector of physical parameters including stiffness, damping and nonlinear model parameters, $\mathbf{R}$ is the total restoring force of the structural system.

Supposing an augmented state vector $\mathbf{Z} = \left\{\mathbf{x}^T, \dot{\mathbf{x}}^T, \boldsymbol{\theta}^T\right\}^T$, Eq. (1) can be converted into the following state space equation as

$$\begin{aligned}\dot{\mathbf{Z}} &= \begin{Bmatrix} \dot{\mathbf{x}} \\ \ddot{\mathbf{x}} \\ \dot{\boldsymbol{\theta}} \end{Bmatrix} = \begin{Bmatrix} \dot{\mathbf{x}} \\ \mathbf{M}^{-1}[\boldsymbol{\eta}\mathbf{f} - \mathbf{R}(\boldsymbol{\theta}, \mathbf{x}, \dot{\mathbf{x}})] \\ \mathbf{0} \end{Bmatrix} + \mathbf{w} \\ &= \mathbf{g}(\mathbf{Z}, \mathbf{f}) + \mathbf{w}\end{aligned} \tag{2}$$

in which $\mathbf{w}$ is the process noise that is assumed to be a Gaussian white noise process with zero mean and a covariance matrix $E[\mathbf{w}\mathbf{w}^T] = \mathbf{Q}$.

Given partially measured acceleration responses, the discrete observation equations is expressed as

$$\begin{aligned}\mathbf{y}_{k+1} &= \ddot{\mathbf{x}}_{m,k+1} = \mathbf{L}_a\ddot{\mathbf{x}}_{k+1} + \mathbf{v}_{k+1} = \mathbf{L}_a\mathbf{M}^{-1} \\ &\quad [\boldsymbol{\eta}\mathbf{f}_{k+1} - \mathbf{R}(\boldsymbol{\theta}_{k+1}, \mathbf{x}_{k+1}, \dot{\mathbf{x}}_{k+1})] + \mathbf{v}_{k+1} \\ &= \mathbf{h}(\mathbf{Z}_{k+1}, \mathbf{f}_{k+1}) + \mathbf{v}_{k+1}\end{aligned} \tag{3}$$

where $\mathbf{y}_{k+1}$ and $\ddot{\mathbf{x}}_{m,k+1}$ represent the observation and the measured acceleration at the time instant $t = (k+1)\Delta t$, respectively, Δt is the sampling interval, $\mathbf{L}_a$ is the accelerometer position matrix and $\mathbf{v}_{k+1}$ is the measurement noise assumed as a Gaussian white noise process, with mean value of zero and covariance matrix of $E\left[\mathbf{v}_{k+1}\mathbf{v}_{k+1}^T\right] = \mathbf{R}_{k+1}$.

Similar as conventional UKF [28], the FUKF method is implemented based on the following procedure, including sigma point calculation, time predication and measurement updating [31].

Sigma point calculation

A set of $2N + 1$ sigma points $\boldsymbol{\chi}_{k|k}$ are generated by using the unscented transform

$$\boldsymbol{\chi}_{i,k|k} = \begin{cases} \hat{\mathbf{Z}}_{k|k}, & i = 0 \\ \hat{\mathbf{Z}}_{k|k} + \left(\sqrt{(N+\vartheta)\hat{\mathbf{P}}_{\mathbf{Z},k|k}}\right)_i, & i = 1,\ldots N \\ \hat{\mathbf{Z}}_{k|k} - \left(\sqrt{(N+\vartheta)\hat{\mathbf{P}}_{\mathbf{Z},k|k}}\right)_i, & i = N+1,\ldots 2N \end{cases} \tag{4}$$

where N is the dimension of $\mathbf{z}$, $\hat{\mathbf{Z}}_{k|k}$ is the estimated state at $t = k\Delta t$, $\hat{\mathbf{P}}_{\mathbf{Z},k|k}$ is the error covariance matrix that is expressed as $\hat{\mathbf{P}}_{\mathbf{Z},k|k} = E\left\{\left(\mathbf{Z}_k - \hat{\mathbf{Z}}_{k|k}\right)\left(\mathbf{Z}_k - \hat{\mathbf{Z}}_{k|k}\right)^T\right\}$, $\vartheta = \kappa_1^2(N+\kappa_2) - N$, κ_1 and κ_2 are scaling parameters determining the spread of the sigma points.

Time predication

The propagation of the sigma points is predicted based on the state space equation

$$\boldsymbol{\chi}_{i,k+1|k} = \boldsymbol{\chi}_{i,k|k} + \int_{k\Delta t}^{(k+1)\Delta t} \mathbf{g}\left(\mathbf{Z}_{t|k}, \mathbf{f}\right) \mathrm{d}t \tag{5}$$

The predicted state vector $\tilde{\mathbf{Z}}_{k+1|k}$ and error covariance matrix $\tilde{\mathbf{P}}_{\mathbf{Z},k+1|k}$ are given as

$$\tilde{\mathbf{Z}}_{k+1|k} = \sum_{i=0}^{2N} W_i^m \boldsymbol{\chi}_{i,k+1|k} \tag{6}$$

$$\tilde{\mathbf{P}}_{\mathbf{Z},k+1|k} = \lambda \sum_{i=0}^{2N} W_i^c (\boldsymbol{\chi}_{i,k+1|k} - \tilde{\mathbf{Z}}_{k+1|k})(\boldsymbol{\chi}_{i,k+1|k} - \tilde{\mathbf{Z}}_{k+1|k})^T + \mathbf{Q}_{k+1} \tag{7}$$

where W_i^m and W_i^c are the weight coefficients of the predicted mean and covariance, respectively. Herein a fading factor $\lambda(\lambda \geq 1)$ is introduced into the conventional UKF. In the first step, $\lambda = 2^{2/N_u}$ is adopted based on an existing study [38], which implies that the half-life of the contribution of a data point is N_u time steps.

Similarly, the estimated measurement vector $\hat{\mathbf{y}}_{k+1|k+1}$ at $t = (k+1)\Delta t$ and its error covariance matrix $\hat{\mathbf{P}}_{\mathbf{y},k+1}$ are computed as

$$\hat{\mathbf{y}}_{i,k+1|k+1} = \mathbf{h}\left(\boldsymbol{\chi}_{i,k+1|k}, \mathbf{f}_{k+1}\right); \hat{\mathbf{y}}_{k+1|k+1} = \sum_{i=0}^{2N} W_i^m \hat{\mathbf{y}}_{i,k+1|k+1} \tag{8}$$

$$\hat{\mathbf{P}}_{\mathbf{y},k+1} = \lambda \sum_{i=0}^{2N} W_i^c (\hat{\mathbf{y}}_{i,k+1|k+1} - \hat{\mathbf{y}}_{k+1|k+1})(\hat{\mathbf{y}}_{i,k+1|k+1} - \hat{\mathbf{y}}_{k+1|k+1})^T + \mathbf{R}_{k+1} \tag{9}$$

Besides, the cross-covariance matrix $\hat{\mathbf{P}}_{\mathbf{Zy},k+1}$ is estimated as

$$\hat{\mathbf{P}}_{\mathbf{Zy},k+1} = \lambda \sum_{i=0}^{2N} W_i^c \left\{\boldsymbol{\chi}_{i,k+1|k} - \tilde{\mathbf{Z}}_{k+1|k}\right\}\left\{\hat{\mathbf{y}}_{i,k+1|k+1} - \hat{\mathbf{y}}_{k+1|k+1}\right\}^T \tag{10}$$

Measurement updating

The structural state vector $\hat{\mathbf{Z}}_{k+1|k+1}$ and error covariance matrix $\hat{\mathbf{P}}_{\mathbf{Z},k+1|k+1}$ are updated as

$$\hat{\mathbf{Z}}_{k+1|k+1} = \tilde{\mathbf{Z}}_{k+1|k} + \mathbf{K}_{G,k+1}(\mathbf{y}_{k+1} - \hat{\mathbf{y}}_{k+1|k+1}) \tag{11}$$

$$\hat{\mathbf{P}}_{\mathbf{Z},k+1|k+1} = \tilde{\mathbf{P}}_{\mathbf{Z},k+1|k} - \mathbf{K}_{G,k+1}\hat{\mathbf{P}}_{\mathbf{y},k+1}\mathbf{K}_{G,k+1}^T \tag{12}$$

in which $\mathbf{K}_{G,k+1}$ is the Kalman gain matrix expressed as

$$\mathbf{K}_{G,k+1} = \hat{\mathbf{P}}_{\mathbf{Zy},k+1}(\hat{\mathbf{P}}_{\mathbf{y},k+1})^{-1} \tag{13}$$

Based on the identification results of FUKF, the physical parameter vector $\boldsymbol{\theta}$ is divided into a time-varying parameter vector $\boldsymbol{\theta}_1$ and a time-invariant parameter vector $\boldsymbol{\theta}_2$ qualitatively. Thus, the time-varying physical parameters can be successfully localized.

2.1.2 *Identify the time-varying physical parameters by the proposed WMA integrated with UKF method*

In the second step, a novel method based on WMA and UKF is proposed to identify $\boldsymbol{\theta}_2$ and scale coefficients corresponding to $\boldsymbol{\theta}_1$ quantitatively.

Wavelet multiresolution analysis

WMA possesses a strong capability in decomposing any signal into approximate and detailed parts in different scale levels, corresponding to the low-frequency and high-frequency components of the signal, respectively [8–12]. Considering that the signal energies in civil engineering are mostly concentrated in the low-frequency component, the time-varying physical parameter $\theta_{1,i}(i = 1, 2, \ldots, m_1)$ is expanded in the

wavelet domain by only reserving the low-frequency part as

$$\theta_{1,i}(t_n) \approx \sum_{l_i} \psi_{J_i,l_i}\phi_{J_i,l_i}(2^{J_i}n - l_i),\ n = 1,2,\ldots,Nt \tag{14}$$

where $\theta_{1,i}$ denotes the ith time-varying parameter, m_1 is the number of time-varying parameters, ψ_{J_i,l_i} is the scale coefficient at the scale level J_i, l_i is the number of corresponding scale coefficients, ϕ_{J_i,l_i} is the scale function in WMA and Nt is the number of sampling points.

Identify structural state by UKF with given scale coefficients and time-invariant physical parameters

By Eq. (14), the time-varying physical parameters can be reconstructed based on the given time-invariant scale coefficient vector $\boldsymbol{\psi}_{J,l}$ accordingly. Thus, it is transformed into the identification of scale coefficients and time-invariant physical parameters. UKF is utilized to estimate the state under the condition of partial acceleration observations. Owning to page limitation, only main formulas are listed in Eqs. (15)–(22).

The equation of motion, state equation and measurement equation of a nonlinear system are rewritten as

$$\mathbf{M}\ddot{\mathbf{x}}(t) + \mathbf{R}\left(\boldsymbol{\theta}_1\left(\boldsymbol{\psi}_{J,l}\right), \boldsymbol{\theta}_2, \mathbf{x}(t), \dot{\mathbf{x}}(t)\right) = \boldsymbol{\eta}\mathbf{f}(t) \tag{15}$$

$$\begin{aligned}\dot{\mathbf{X}} &= \begin{Bmatrix}\dot{\mathbf{x}}\\ \ddot{\mathbf{x}}\end{Bmatrix}\\ &= \begin{Bmatrix}\dot{\mathbf{x}}\\ \mathbf{M}^{-1}\left[\boldsymbol{\eta}\mathbf{f} - \mathbf{R}\left(\boldsymbol{\theta}_1\left(\boldsymbol{\psi}_{J,l}\right), \boldsymbol{\theta}_2, \mathbf{x}, \dot{\mathbf{x}}\right)\right]\end{Bmatrix} + \mathbf{w}\\ &= \mathbf{g}\left(\mathbf{X}, \boldsymbol{\theta}_1\left(\boldsymbol{\psi}_{J,l}\right), \boldsymbol{\theta}_2, \mathbf{f}\right) + \mathbf{w}\end{aligned} \tag{16}$$

$$\begin{aligned}\mathbf{y}_{k+1} &= \ddot{\mathbf{x}}_{m,k+1} = \mathbf{L}_a\ddot{\mathbf{x}}_{k+1} + \mathbf{v}_{k+1}\\ &= \mathbf{L}_a\mathbf{M}^{-1}\left[\boldsymbol{\eta}\mathbf{f}_{k+1} - \mathbf{R}\left(\boldsymbol{\theta}_1\left(\boldsymbol{\psi}_{J,l}\right), \boldsymbol{\theta}_2, \mathbf{x}_{k+1}, \dot{\mathbf{x}}_{k+1}\right)\right] + \mathbf{v}_{k+1}\\ &= \mathbf{h}\left(\mathbf{X}_{k+1}, \boldsymbol{\theta}_1\left(\boldsymbol{\psi}_{J,l}\right), \boldsymbol{\theta}_2, \mathbf{f}_{k+1}\right) + \mathbf{v}_{k+1}\end{aligned} \tag{17}$$

The predicted state vector $\tilde{\mathbf{X}}_{k+1|k}$ and error covariance matrix $\tilde{\mathbf{P}}_{\mathbf{X},k+1|k}$ are given as

$$\begin{aligned}\boldsymbol{\chi}_{i,k+1|k} &= \boldsymbol{\chi}_{i,k|k} + \int_{k\Delta t}^{(k+1)\Delta t} \mathbf{g}\left(\mathbf{X}_{t|k}, \boldsymbol{\theta}_1\left(\boldsymbol{\psi}_{J,l}\right), \boldsymbol{\theta}_2, \mathbf{f}\right)\mathrm{d}t;\quad \tilde{\mathbf{X}}_{k+1|k}\\ &= \sum_{i=0}^{2N} W_i^m \boldsymbol{\chi}_{i,k+1|k}\end{aligned} \tag{18}$$

$$\begin{aligned}\tilde{\mathbf{P}}_{\mathbf{X},k+1|k} = \sum_{i=0}^{2N} W_i^c(\boldsymbol{\chi}_{i,k+1|k} - \tilde{\mathbf{X}}_{k+1|k})(\boldsymbol{\chi}_{i,k+1|k}\\ - \tilde{\mathbf{X}}_{k+1|k})^T + \mathbf{Q}_{k+1}\end{aligned} \tag{19}$$

The estimated measurement vector $\hat{\mathbf{y}}_{k+1|k+1}$, its error covariance matrix $\hat{\mathbf{P}}_{\mathbf{y},k+1}$ and the cross-covariance matrix $\hat{\mathbf{P}}_{\mathbf{Xy},k+1}$ are rewritten as

$$\begin{aligned}\hat{\mathbf{y}}_{i,k+1|k+1} &= \mathbf{h}\left(\boldsymbol{\chi}_{i,k+1|k}, \boldsymbol{\theta}_1\left(\boldsymbol{\psi}_{J,l}\right), \boldsymbol{\theta}_2, \mathbf{f}_{k+1}\right); \hat{\mathbf{y}}_{k+1|k+1}\\ &= \sum_{i=0}^{2N} W_i^m \hat{\mathbf{y}}_{i,k+1|k+1}\end{aligned} \tag{20}$$

$$\begin{aligned}\hat{\mathbf{P}}_{\mathbf{y},k+1} = \sum_{i=0}^{2N} W_i^c(\hat{\mathbf{y}}_{i,k+1|k+1} - \hat{\mathbf{y}}_{k+1|k+1})(\hat{\mathbf{y}}_{i,k+1|k+1}\\ - \hat{\mathbf{y}}_{k+1|k+1})^T + \mathbf{R}_{k+1}\end{aligned} \tag{21}$$

$$\hat{\mathbf{P}}_{\mathbf{Xy},k+1} = \sum_{i=0}^{2N} W_i^c\left\{\boldsymbol{\chi}_{i,k+1|k} - \tilde{\mathbf{X}}_{k+1|k}\right\}\left\{\hat{\mathbf{y}}_{i,k+1|k+1} - \hat{\mathbf{y}}_{k+1|k+1}\right\}^T \tag{22}$$

Finally, the structural state vector and error covariance matrix in Eqs. (11) and (12) are updated, respectively.

Estimate scale coefficients and time-invariant physical parameters by nonlinear optimization

As can be seen from the above sections, the estimated state is an implicit function of the scale coefficient vector $\boldsymbol{\psi}_{J,l}$ and time-invariant physical parameter vector $\boldsymbol{\theta}_2$,

$$\hat{\mathbf{X}} = \hat{\mathbf{X}}\left(\boldsymbol{\psi}_{J,l}, \boldsymbol{\theta}_2\right) \tag{23}$$

Then, the estimated acceleration is obtained by using the equation of motion in Eq. (15)

$$\hat{\ddot{\mathbf{x}}}\left(\boldsymbol{\psi}_{J,l}, \boldsymbol{\theta}_2\right) = \mathbf{M}^{-1}\left(\boldsymbol{\eta}\mathbf{f} - \mathbf{R}\left(\boldsymbol{\theta}_1\left(\boldsymbol{\psi}_{J,l}\right), \boldsymbol{\theta}_2, \hat{\mathbf{X}}\left(\boldsymbol{\psi}_{J,l}, \boldsymbol{\theta}_2\right), \hat{\dot{\mathbf{x}}}\left(\boldsymbol{\psi}_{J,l}, \boldsymbol{\theta}_2\right)\right)\right) \tag{24}$$

An objective error function is established by integrating the observed acceleration $\ddot{\mathbf{x}}_m$ and the estimated acceleration $\hat{\ddot{\mathbf{x}}}$ as

$$\Delta\left(\boldsymbol{\psi}_{J,l},\boldsymbol{\theta}_2\right)=\left\|\ddot{\mathbf{x}}_m-\mathbf{L}_a\hat{\ddot{\mathbf{x}}}\left(\boldsymbol{\psi}_{J,l},\boldsymbol{\theta}_2\right)\right\|_2^2 \tag{25}$$

The optimal scale coefficient vector $\widehat{\boldsymbol{\psi}}_{J,l}$ and optimal time-invariant physical parameter vector $\widehat{\boldsymbol{\theta}}_2$ are calculated by minimizing the objective error function

$$\left[\widehat{\boldsymbol{\psi}}_{J,l},\widehat{\boldsymbol{\theta}}_2\right]=\arg\min_{\boldsymbol{\psi}_{J,l},\boldsymbol{\theta}_2}\left(\left\|\ddot{\mathbf{x}}_m-\mathbf{L}_a\hat{\ddot{\mathbf{x}}}\left(\boldsymbol{\psi}_{J,l},\boldsymbol{\theta}_2\right)\right\|_2^2\right) \tag{26}$$

Finally, the optimal time-varying physical parameter vector $\widehat{\boldsymbol{\theta}}_1$ is reconstructed by using the inverse WMA in Eq. (14).

The procedure of the proposed method is listed in Fig. 1.

2.2 Numerical verification: identification of a time-varying nonlinear six-story shear frame subjected to a known seismic acceleration

The first numerical example is a six-story shear frame with a Bouc–Wen model subjected to the 1940 El Centro N-S earthquake with the peak value scaled to 0.4 g. The equation of motion of the structure is given as

$$\mathbf{M}\ddot{\mathbf{x}}(t)+\mathbf{C}(t)\dot{\mathbf{x}}(t)+\mathbf{K}(t)\mathbf{z}(t)=-\mathbf{M}\{\mathbf{I}\}\ddot{x}_g(t) \tag{27}$$

where $\mathbf{C}$ and $\mathbf{K}$ are global damping and stiffness matrices which are composed of the unknown time-varying damping and stiffness parameters, $\{\mathbf{I}\}$ is a unit vector and $\ddot{x}_g(t)$ is the base acceleration. $\mathbf{z}(t)$ is the

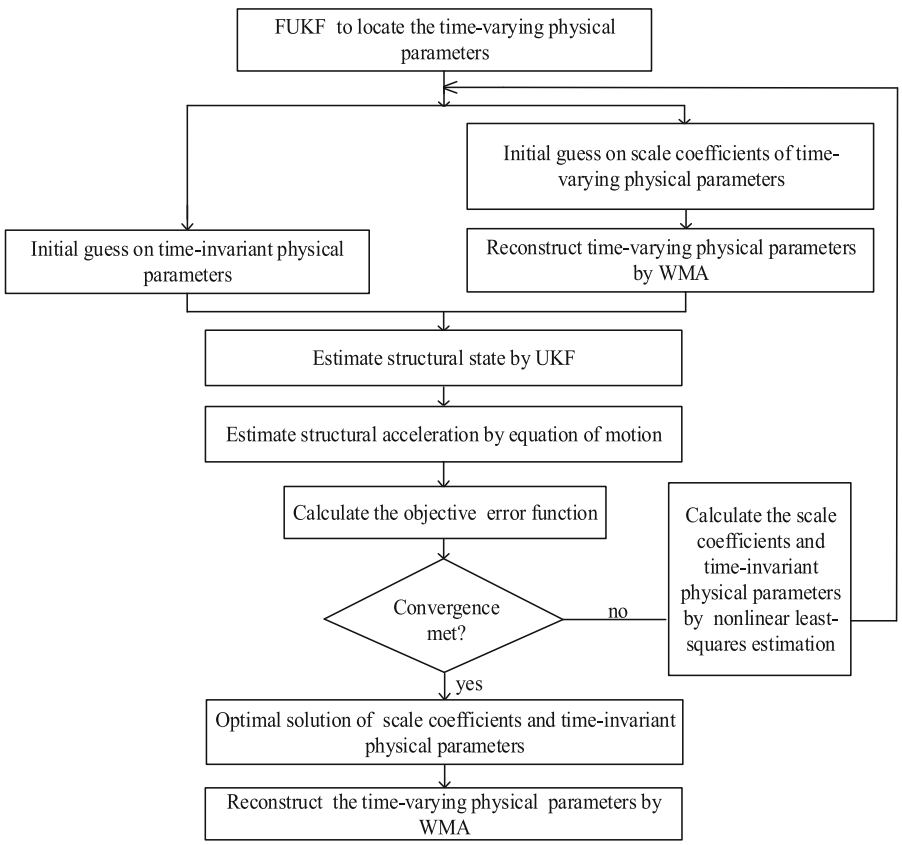

Fig. 1 Procedure of the proposed method to identify the time-varying nonlinear structures with a small number of elements under known excitation

hysteretic displacement vector with the specific expression as follows

$$\dot{z}_i = \dot{x}_i - \dot{x}_{i-1} - \beta_i|\dot{x}_i - \dot{x}_{i-1}||z_i|^{n_i-1}\dot{z}_i - \gamma_i(\dot{x}_i - \dot{x}_{i-1})|\dot{z}_i|^{n_i}, \quad (i = 1, 2, \ldots, 6) \tag{28}$$

where n_i, β_i and γ_i $(i = 1, 2, \cdots, 6)$ are parameters for the Bouc–Wen hysteretic model. It is assumed that the nonlinear damage occurs with the restoring force between the first floor and the ground following the Bouc–Wen model. It should be noted that the Bouc–Wen model is adopted here only as an example to illustrate the proposed method. The proposed approach can be applied to identify structural physical parameters with different nonlinear response characteristics.

Structural parameters are selected as follows: the mass of each story and the Bouc–Wen hysteretic model parameter n_1 are assumed to be known as $m_i = 200$ kg $(i = 1, 2\ldots, 6)$ and $n_1 = 1.8$. The corresponding dynamic responses are computed with a sampling frequency of 50 Hz, and the complete sampling period is 10 s. The acceleration measurements at the 1st, 3rd and 5th floors are used. Each measured response is polluted by white noise with 2% variance in root mean square (RMS), namely:

$$\ddot{\mathbf{x}}_{i,\text{noisy}} = \ddot{\mathbf{x}}_{i,\text{clean}} + 2\% \times \text{std}\left(\ddot{\mathbf{x}}_{i,\text{clean}}\right) \times \mathbf{rand}, \ (i = 1, 3, 5) \tag{29}$$

where $\ddot{\mathbf{x}}_{i,\text{noisy}}$ is the measured noisy acceleration vector, $\ddot{\mathbf{x}}_{i,\text{clean}}$ is the noisy-free acceleration vector, $\text{std}\left(\ddot{\mathbf{x}}_{i,\text{clean}}\right)$ means the standard deviation of $\ddot{\mathbf{x}}_{i,\text{clean}}$ and **rand** is a random standard normal distribution vector.

The stiffness, viscous damping parameters of each story $k_i, c_i (i = 1, 2\ldots, 6)$, and the Bouc–Wen hysteretic model parameters β and γ need to be identified. Two cases are discussed here.

2.2.1 *Case I: Identification of abruptly changing physical parameters*

The theoretical values of the physical parameters in case I are given below:

Fig. 2 Identification results using the FUKF method in case I. **a** ▶ k_1; **b** k_2; **c** k_3; **d** k_4; **e** k_5; **f** k_6; **g** c_1; **h** c_2; **i** c_3; **j** c_4; **k** c_5; **l** c_6; **m** β_1; **n** γ_1

$$k_1 = \begin{cases} 1.0 \times 10^5 \text{ N/m}, & 0\text{s} \le t < 5.2\text{s} \\ 0.8 \times 10^5 \text{ N/m}, & 5.2\text{s} \le t \le 10\text{s} \end{cases}$$

$$k_i = 1.5 \times 10^5 \text{ N/m}, \quad 0\text{s} \le t \le 10\text{s} (i = 2, \ldots, 6)$$

$$c_1 = \begin{cases} 800 \text{ N} \cdot \text{s/m}, & 0\text{s} \le t < 5.2\text{s} \\ 1120 \text{ N} \cdot \text{s/m}, & 5.2\text{s} \le t \le 10\text{s} \end{cases}$$

$$c_i = 1000 \text{ N} \cdot \text{s/m}, \quad 0\text{s} \le t \le 10\text{s} (i = 2, \ldots, 6)$$

$$\beta_1 = \begin{cases} 600, & 0s \le t < 5.2s \\ 780, & 5.2s \le t \le 10\text{s} \end{cases}$$

$$\gamma_1 = 600, \quad 0s \le t \le 10\text{s}$$

Referring to the flowchart in Fig. 1, the identification process is accomplished by the following procedure. Firstly, the time-varying physical parameters are distinguished using the FUKF method, which is shown in Fig. 2. $\lambda = 2^{2/30} = 1.0473$ is used, which indicates the half-life is 30 time steps. It can be seen from Fig. 2 that stiffness parameter k_1 changes gradually from a stable converged value to another stable converged value, implying that k_1 may be a time-varying physical parameter. Similarly, c_1 has the tendency to increase, which can also be selected as another time-varying physical parameter. However, the FUKF method can only roughly determine these physical parameters with the time-varying properties, but it is unable to detect the time-varying instant, time-varying trend and time-varying degree.

Secondly, the proposed WMA integrated with the UKF method is applied to conduct the identification of time-varying physical parameters. Following the experience in an existing study by Chang and Shi [27], Db1 is adopted herein as the wavelet function to expand the time-varying k_1, c_1, and nonlinear model parameters β_1 and γ_1. The scale level is $J = 7$. The number of scale coefficients is 16 in total. The remaining five time-invariant stiffness parameters and five time-invariant damping parameters are not expanded by the WMA, and they are directly included in the nonlinear optimization process.

Figures 3, 4 and 5 show the identified physical parameters with comparisons to their exact values, respectively. It can be seen from Figs. 3 and 4 that the proposed WMA integrated with the UKF method can

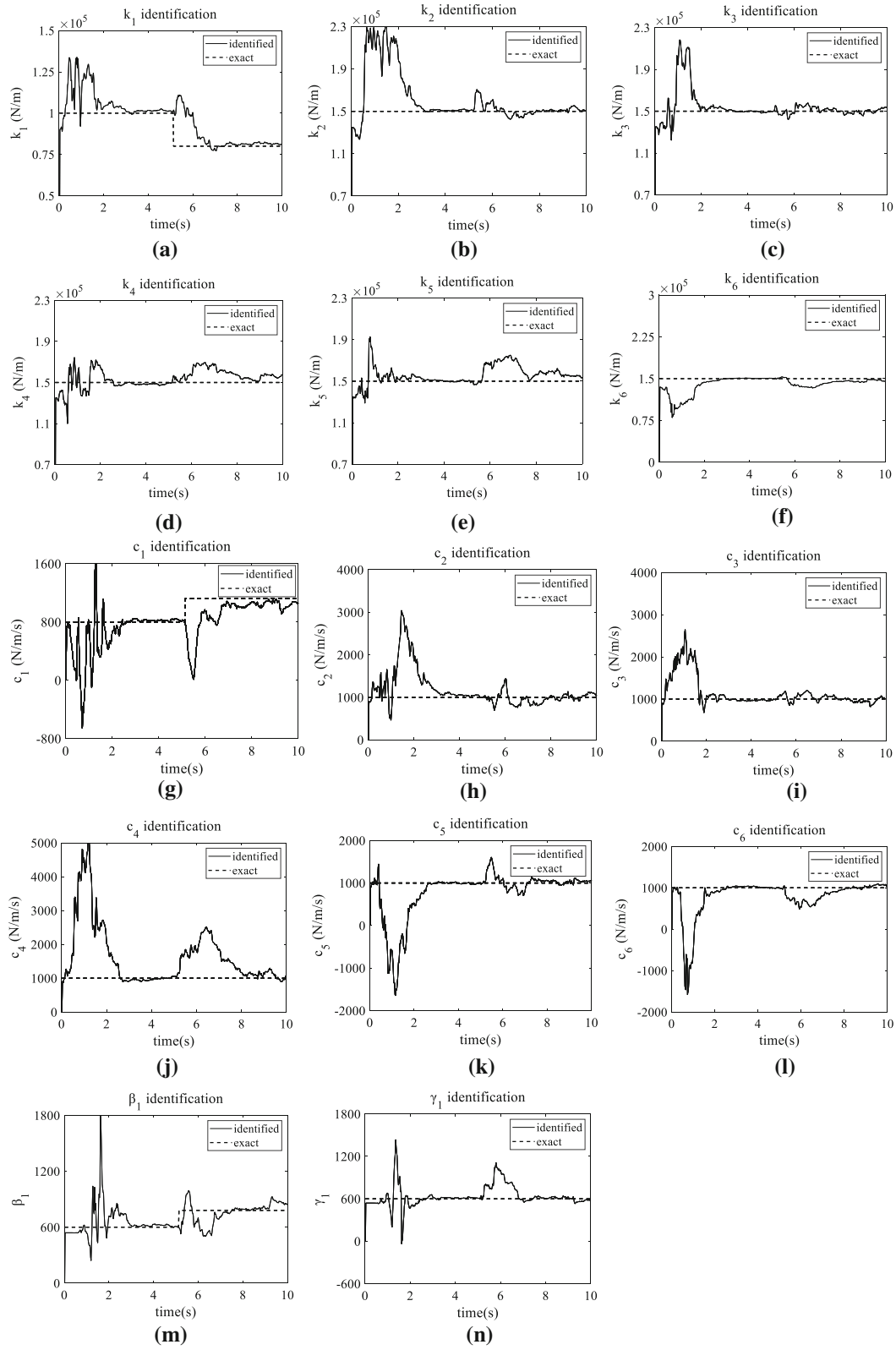
k1 identification
k2 identification
k3 identification
k4 identification
k5 identification
k6 identification
c1 identification
c2 identification
c3 identification
c4 identification
c5 identification
c6 identification
β1 identification
γ1 identification
identified
exact
time(s)
(a)
(b)
(c)
(d)
(e)
(f)
(g)
(h)
(i)
(j)
(k)
(l)
(m)
(n)

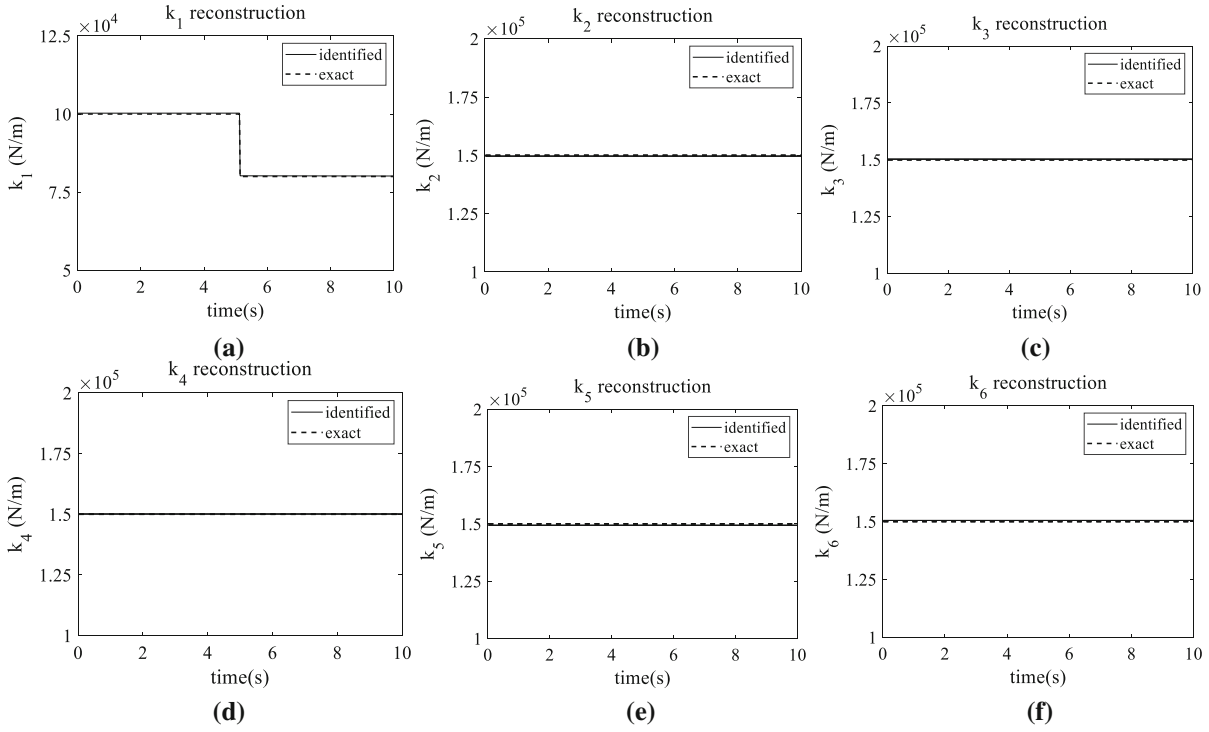

Fig. 3 Comparison of the exact and identified stiffness parameters in case I. **a** k_1; **b** k_2; **c** k_3; **d** k_4; **e** k_5; **f** k_6

precisely track the sudden change of stiffness and damping parameters, and the identification of time-invariant parameters also shows a high precision. Figure 5 shows that the proposed method is also effective in identifying the time-varying nonlinear model parameters. It is noted that the desirable results are achieved by using only three noisy acceleration responses.

2.2.2 *Case II: Identification of gradually varying physical parameters*

The theoretical values of the physical parameters in case II are shown below, in which k_1 is gradually varying and expressed as

$$k_1 = \begin{cases} 1.0 \times 10^5 \text{ N/m}, & 0\text{s} \le t < 2\text{s} \\ -5360t + 1.1 \times 10^5 \text{ (N/m)}, & 2\text{s} \le t \le 7.6\text{s} \\ 0.7 \times 10^5 \text{N/m}, & 7.6\text{s} < t \le 10\text{s} \end{cases}$$

$$k_i = 1.5 \times 10^5 \text{ N/m}, \quad 0\text{s} \le t \le 10\text{s} (i = 2, \ldots, 6)$$

$$c_1 = 800 \text{ N} \cdot \text{s/m}, 0\text{s} \le t \le 10\text{s}$$

$$c_i = 1000 \text{ N} \cdot \text{s/m}, 0\text{s} \le t \le 10\text{s} (i = 2, \ldots, 6)$$

$$\beta_1 = \begin{cases} 600, & 0\text{s} \le t < 5.2\text{s} \\ 780, & 5.2\text{s} \le t \le 10\text{s} \end{cases}$$

$$\gamma_1 = 600, \quad 0\text{s} \le t \le 10\text{s}$$

The time-varying physical parameters are roughly located using the FUKF method. For brevity and without losing generality, only the partial identification results are shown in Fig. 6. It is observed that the identified value of k_1 tends to change gradually, while other stiffness and damping parameters converge to fixed values. However, it should be noted that a relatively large error may be present at the start and end time instants.

The gradually varying k_1 is expanded using the wavelet function Db3 with the scale level $J = 5$ suggested by Chang and Shi [27]. The time-varying

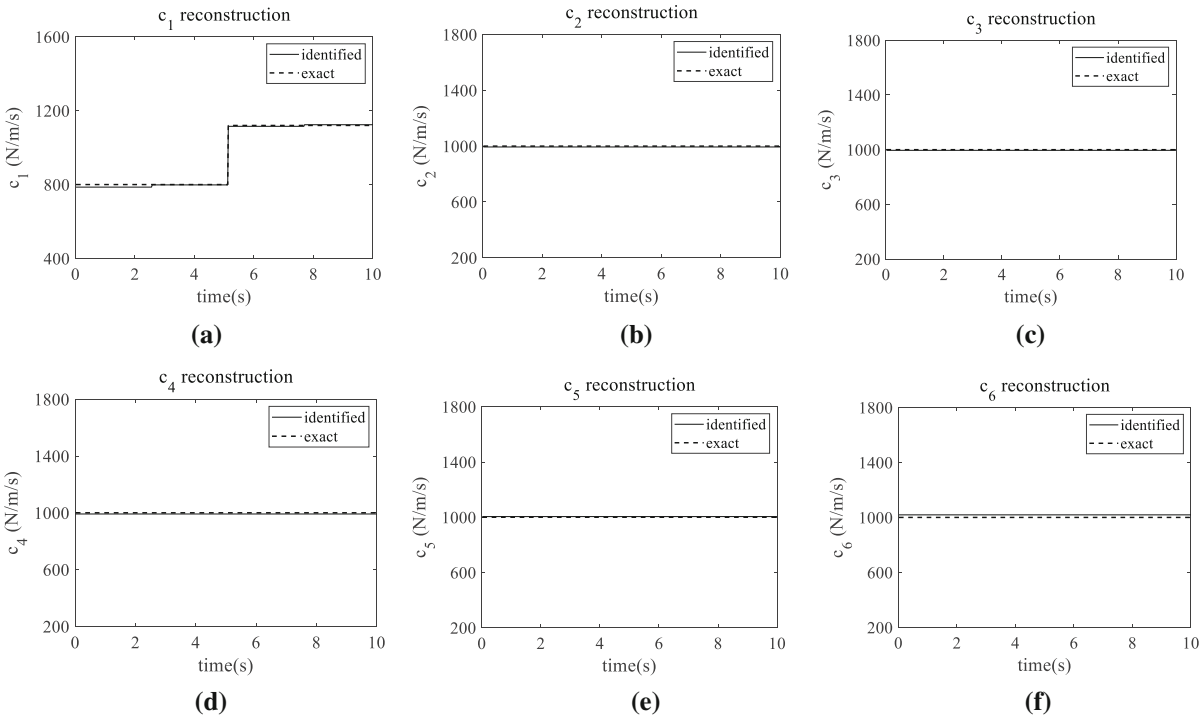

Fig. 4 Comparison of the exact and identified damping parameters in case I. **a** c_1; **b** c_2; **c** c_3; **d** c_4; **e** c_5; **f** c_6

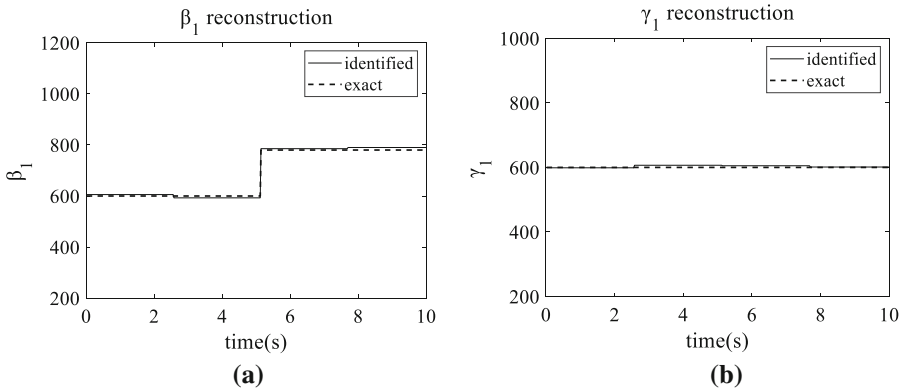

Fig. 5 Comparison of the exact and identified nonlinear model parameters in case I. **a** β_1; **b** γ_1

nonlinear model parameters β_1 and γ_1 are also expanded using the wavelet function Db1 with the scale level $J = 7$. Thus, the variables involved in the nonlinear optimization include 24 scale coefficients and 11 time-invariant physical parameters. The identification results are shown in Figs. 7, 8 and 9, demonstrating that the proposed method is also suitable for the identification of gradually changing parameters in the presence of measurement noise. It not only effectively detects the start and end time of the gradual change, but also accurately identifies the degree of the varying parameters. Meanwhile, the identified time-invariant physical parameters are in good agreement with the exact values.

3 Identification of time-varying nonlinear structures with a small number of elements under unknown excitations

It shall be noted that the proposed method in Sect. 2 is only applicable for the case of known excitations,

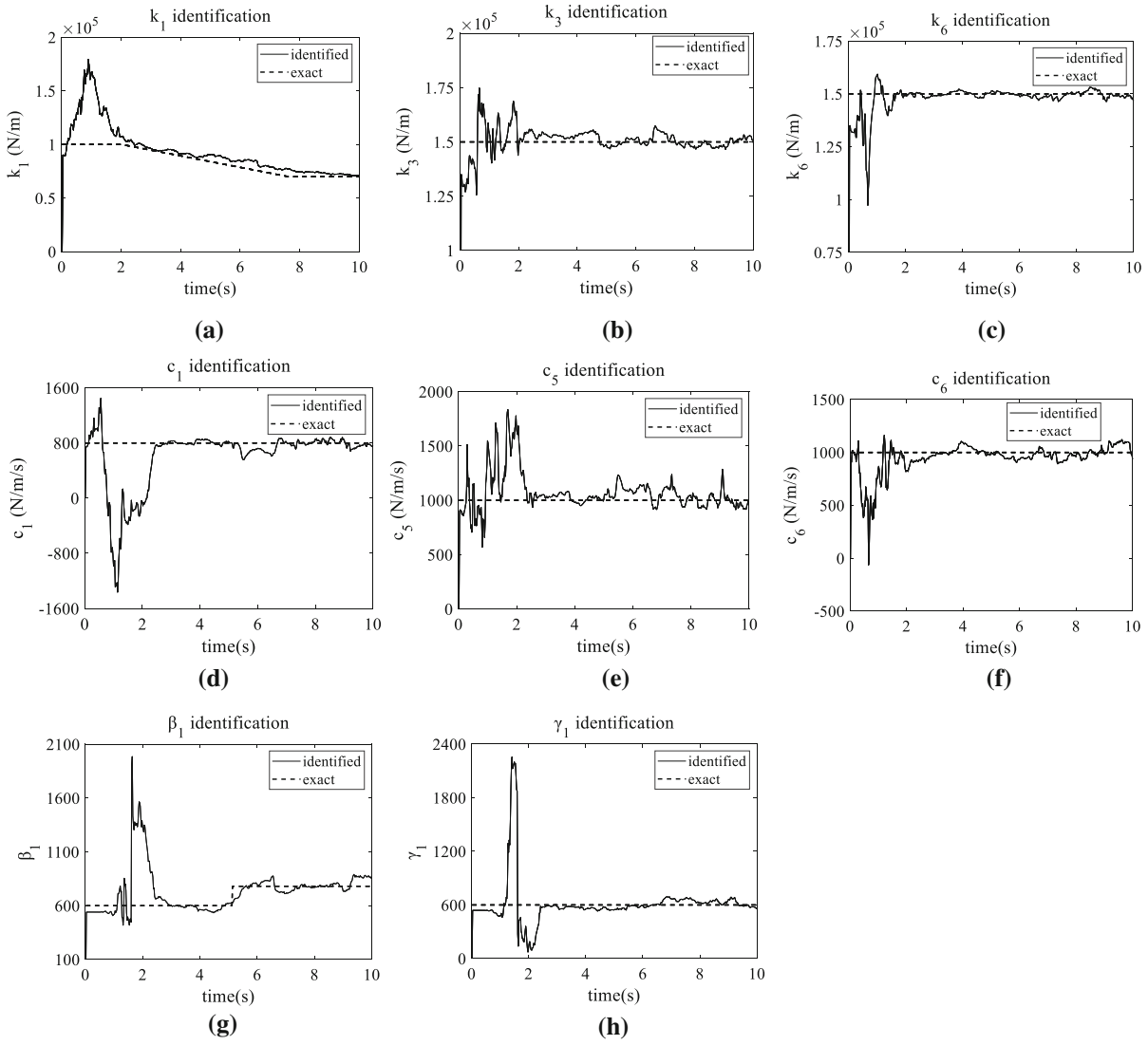

Fig. 6 Partial identification results using the FUKF method in case II. **a** k_1; **b** k_3; **c** k_6; **d** c_1; **e** c_5; **f** c_6; **g** β_1; **h** γ_1

owning to the limitation of UKF itself. However, external excitations could not be always measured directly and easily in practical engineering applications. To further generalize the application to a more common case, the identification of time-varying nonlinear structures with a small number of elements but under unknown excitations is discussed in this section.

3.1 The proposed two-step identification process

3.1.1 Locate the time-varying physical parameters by the proposed FUKF-UI method

In this section, the method introduced in Sect. 2.1.1 is further extended to locate the time-varying physical parameters under unknown excitations. A new method, that is fading-factor unscented Kalman filter under unknown input, is proposed. It is also an improvement for the data fusion-based UKF-UI proposed by the authors in 2019 [30], for the reason

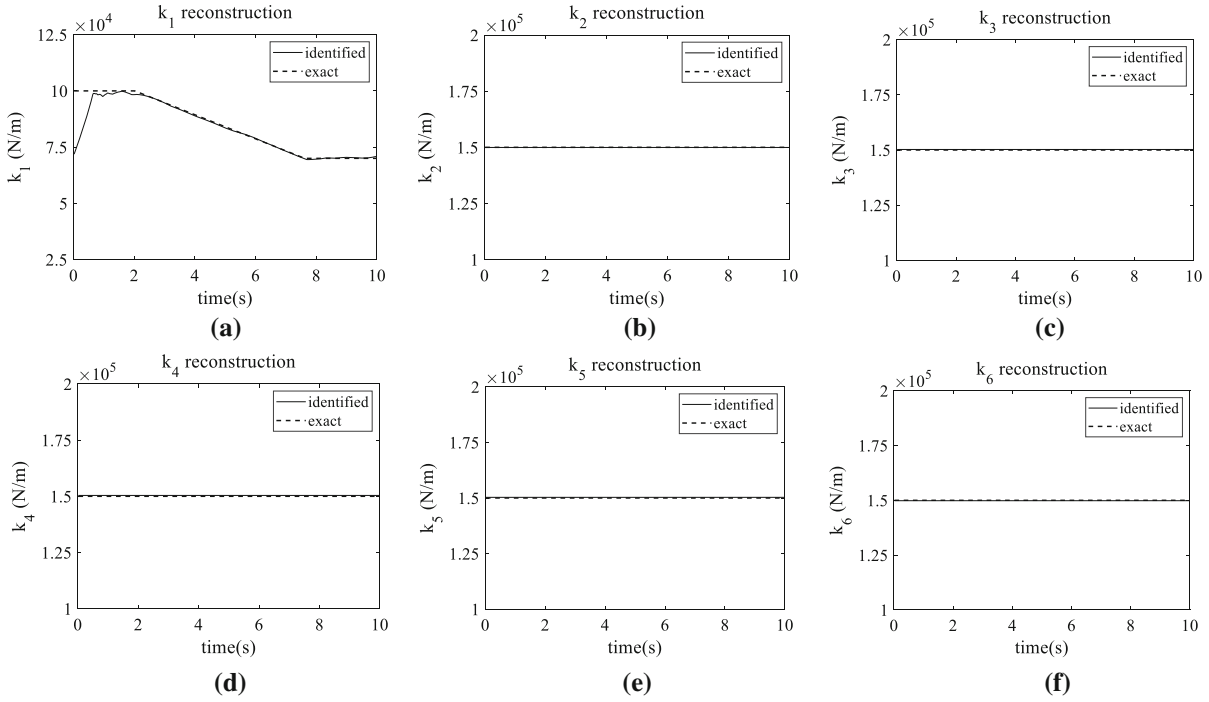

Fig. 7 Comparison of the exact and identified stiffness parameters in case II. **a** k_1; **b** k_2; **c** k_3; **d** k_4; **e** k_5; **f** k_6

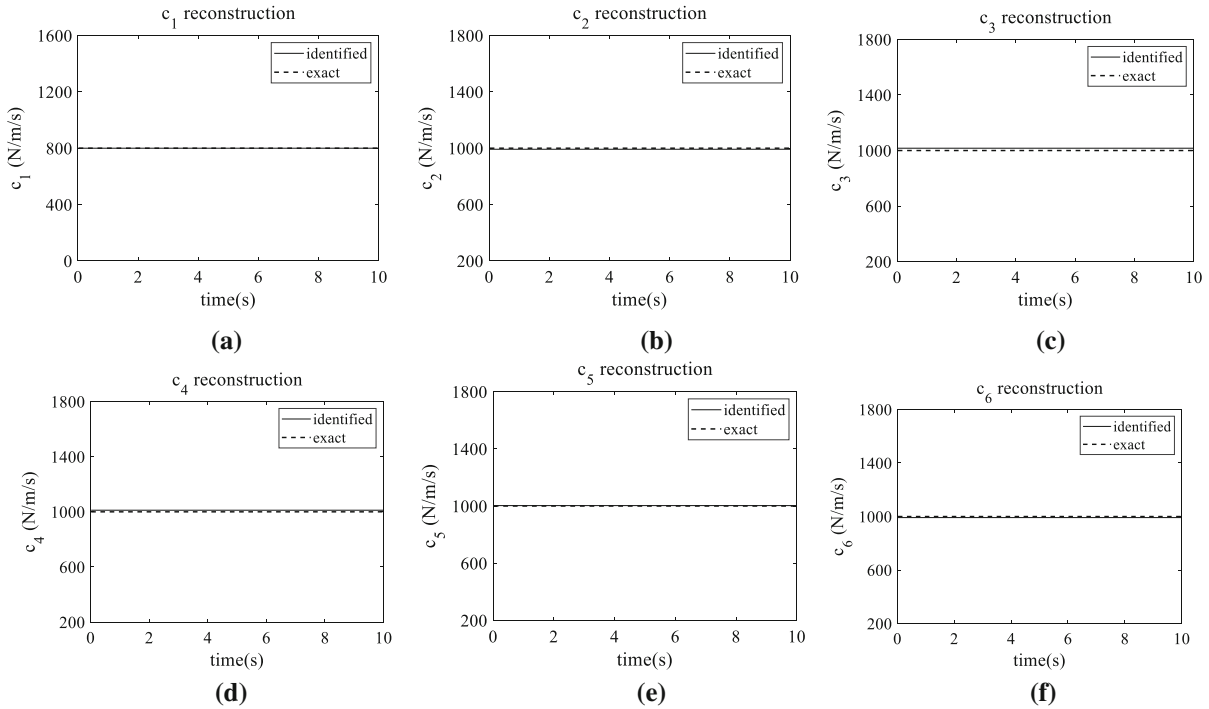

Fig. 8 Comparison of the exact and identified damping parameters in case II. **a** c_1; **b** c_2; **c** c_3; **d** c_4; **e** c_5; **f** c_6

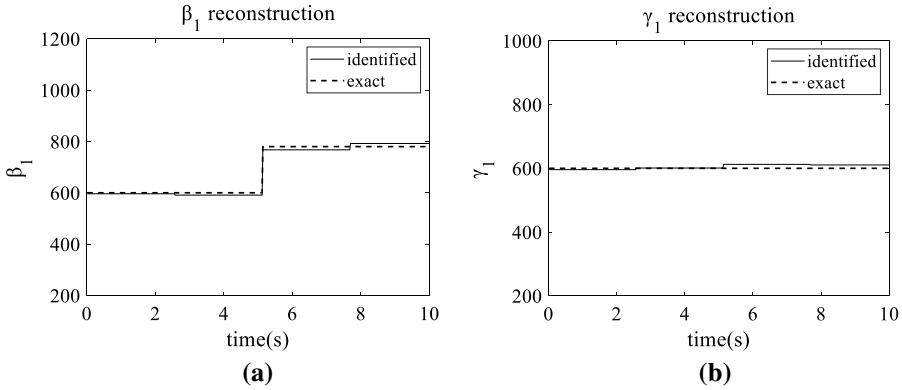

Fig. 9 Comparison of the exact and identified nonlinear model parameters in case II. **a** β_1; **b** γ_1

that the latter is only available for the identification of time-invariant systems under the condition of unknown excitations.

If partial external inputs to the time-varying nonlinear structure are unknown, the equation of motion in Eq. (1) can be rewritten as

$$\mathbf{M}\ddot{\mathbf{x}}(t) + \mathbf{R}(\boldsymbol{\theta}(t), \mathbf{x}(t), \dot{\mathbf{x}}(t)) = \boldsymbol{\eta}\mathbf{f}(t) + \boldsymbol{\eta}^u\mathbf{f}^u(t) \tag{30}$$

where $\mathbf{f}^u$ denotes the unknown input vector with the corresponding influence matrix $\boldsymbol{\eta}^u$. The state space equation can be expressed as

$$\begin{aligned}\dot{\mathbf{Z}} &= \begin{Bmatrix} \dot{\mathbf{x}} \\ \ddot{\mathbf{x}} \\ \dot{\boldsymbol{\theta}} \end{Bmatrix} \\ &= \begin{Bmatrix} \dot{\mathbf{x}} \\ \mathbf{M}^{-1}[\boldsymbol{\eta}\mathbf{f} - \mathbf{R}(\boldsymbol{\theta}, \mathbf{x}, \dot{\mathbf{x}})] \\ \mathbf{0} \end{Bmatrix} + \begin{Bmatrix} \mathbf{0} \\ \mathbf{M}^{-1}\boldsymbol{\eta}^u \\ \mathbf{0} \end{Bmatrix}\mathbf{f}^u + \mathbf{w} \\ &= \mathbf{g}(\mathbf{Z}, \mathbf{f}) + \boldsymbol{\varphi}^u\mathbf{f}^u + \mathbf{w}\end{aligned} \tag{31}$$

where $\boldsymbol{\varphi}^u$ is the influence matrix related to the unknown input $\mathbf{f}^u$ in the above equation.

It should be emphasized that the partially measured acceleration and displacement responses are used in the data fusion based UKF-UI as an on-line technique to restrain the "drift" in the identification results [30]. Thus, the observation equation in the discrete form is given as

$$\begin{aligned}\mathbf{y}_{k+1} &= \begin{bmatrix} \ddot{\mathbf{x}}_{m,k+1} \\ \mathbf{x}_{m,k+1} \end{bmatrix} = \begin{bmatrix} \mathbf{L}_a & \mathbf{0} \\ \mathbf{0} & \mathbf{L}_d \end{bmatrix} \\ &\begin{bmatrix} \mathbf{M}^{-1}[\boldsymbol{\eta}\mathbf{f}_{k+1} - \mathbf{R}(\boldsymbol{\theta}_{k+1}, \mathbf{x}_{k+1}, \dot{\mathbf{x}}_{k+1})] \\ \dot{\mathbf{x}}_{k+1} \end{bmatrix} \\ &+ \begin{bmatrix} \mathbf{L}_a\mathbf{M}^{-1}\boldsymbol{\eta}^u\mathbf{f}^u_{k+1} \\ \mathbf{0} \end{bmatrix} + \mathbf{v}_{k+1} \\ &= \mathbf{h}(\mathbf{Z}_{k+1}, \mathbf{f}_{k+1}) + \boldsymbol{\lambda}^u\mathbf{f}^u_{k+1} + \mathbf{v}_{k+1}\end{aligned} \tag{32}$$

where $\mathbf{x}_{m,k+1}$ is the measured displacement at $t = (k+1)\Delta t$ with the position matrix $\mathbf{L}_d$ and $\boldsymbol{\lambda}^u$ is the influence matrix.

The proposed FUKF-UI has a similar process with FUKF. Only the main formulas are briefly presented here.

Sigma point calculation

The same set of sigma points $\boldsymbol{\chi}_{k|k}$ are generated as shown in Eq. (4).

Time predication

Under the premise of zero-order hold (ZOH), the propagation of the sigma points at $t = (k+1)\Delta t$ is expressed as

$$\boldsymbol{\chi}_{i,k+1|k} = \boldsymbol{\chi}_{i,k|k} + \int_{k\Delta t}^{(k+1)\Delta t} \mathbf{g}(\boldsymbol{\chi}_{i,t|k}, \mathbf{f})\mathrm{d}t + \boldsymbol{\varphi}^u\mathbf{f}^u_{k|k}\Delta t \tag{33}$$

The predicted state vector $\tilde{\mathbf{Z}}_{k+1|k}$ and its error covariance matrix $\tilde{\mathbf{P}}_{\mathbf{Z},k+1|k}$ are provided by the same formulas in Eqs. (6) and (7), respectively.

The estimated measurement vector $\hat{\mathbf{y}}_{k+1|k+1}$ at $t = (k+1)\Delta t$ is given as

$$\hat{\mathbf{y}}_{k+1|k+1} = \sum_{i=0}^{2N} W_i^m \left[\mathbf{h}\left(\boldsymbol{\chi}_{i,k+1|k}, \mathbf{f}_{k+1}\right)\right] + \boldsymbol{\lambda}^u \hat{\mathbf{f}}^u_{k+1|k+1} \tag{34}$$

The error covariance matrix of measurement vector $\hat{\mathbf{P}}_{\mathbf{y},k+1}$ and the cross-covariance matrix $\hat{\mathbf{P}}_{\mathbf{Z}\mathbf{y},k+1}$ are found in Eqs. (9) and (10), respectively.

Unknown input calculation

The state vector is updated by Eq. (11), which is workable only when the unknown input $\hat{\mathbf{f}}^u_{k+1|k+1}$ is given for the reason that $\hat{\mathbf{y}}_{k+1|k+1}$ is a function of $\hat{\mathbf{f}}^u_{k+1|k+1}$, as shown in Eq. (34). To solve the unknown force $\hat{\mathbf{f}}^u_{k+1|k+1}$, the estimated state vector $\hat{\mathbf{Z}}_{k+1|k+1}$ in Eq. (11) is substituted into the measurement equation

$$\hat{\mathbf{y}}_{k+1|k+1} = \mathbf{h}\left(\hat{\mathbf{Z}}_{k+1|k+1}, \mathbf{f}_{k+1}\right) + \boldsymbol{\lambda}^u \hat{\mathbf{f}}^u_{k+1|k+1} \tag{35}$$

Then, an estimation error function is established between the real measurement and the estimated measurement as

$$\Delta_{k+1} = \mathbf{y}_{k+1} - \mathbf{h}\left(\hat{\mathbf{Z}}_{k+1|k+1}, \mathbf{f}_{k+1}\right) - \boldsymbol{\lambda}^u \hat{\mathbf{f}}^u_{k+1|k+1} \tag{36}$$

Under the condition that the number of observed measurements is larger than that of the unknown excitations, $\hat{\mathbf{f}}^u_{k+1|k+1}$ can be computed by minimizing the error Δ_{k+1} in Eq. (36) by solving a nonlinear least-squares problem.

Measurement updating

Once $\hat{\mathbf{f}}^u_{k+1|k+1}$ is obtained, the estimated measurement vector $\hat{\mathbf{y}}_{k+1|k+1}$ can be calculated with Eq. (34). Then, the estimated state vector $\hat{\mathbf{Z}}_{k+1|k+1}$ is solved by Eq. (11). Finally, the error covariance matrix $\hat{\mathbf{P}}_{\mathbf{Z},k+1|k+1}$ is updated using Eq. (12).

3.1.2 Identify the time-varying physical parameters by the proposed WMA integrated with UKF-UI method

After the qualitative analysis of time-varying physical parameters under unknown excitations by FUKF-UI, a new method is proposed for quantitative identification of time-varying parameters, which combines the advantage of WMA and UKF-UI under unknown excitations.

The proposed WMA integrated with UKF-UI method has a similar process as WMA integrated with the UKF method presented in Sect. 2.1.2. Firstly, the time-varying physical parameters distinguished in the first step can be reconstructed based on the given time-invariant scale coefficient vector $\boldsymbol{\psi}_{J,l}$ in Eq. (14). Then with the initial time-invariant physical parameter vector $\boldsymbol{\theta}_2$, UKF-UI is applied to obtain the estimated state and input following Eqs. (37)–(41).

The equation of motion, state equation and measurement equation of a nonlinear system under unknown excitations are rewritten as

$$\mathbf{M}\ddot{\mathbf{x}}(t) + \mathbf{R}\left(\boldsymbol{\theta}_1\left(\boldsymbol{\psi}_{J,l}\right), \boldsymbol{\theta}_2, \mathbf{x}(t), \dot{\mathbf{x}}(t)\right) = \boldsymbol{\eta}\mathbf{f}(t) + \boldsymbol{\eta}^u \mathbf{f}^u(t) \tag{37}$$

$$\dot{\mathbf{X}} = \begin{Bmatrix} \dot{\mathbf{x}} \\ \ddot{\mathbf{x}} \end{Bmatrix} = \begin{Bmatrix} \dot{\mathbf{x}} \\ \mathbf{M}^{-1}\left[\boldsymbol{\eta}\mathbf{f} - \mathbf{R}\left(\boldsymbol{\theta}_1\left(\boldsymbol{\psi}_{J,l}\right), \boldsymbol{\theta}_2, \mathbf{x}, \dot{\mathbf{x}}\right)\right] \end{Bmatrix} + \begin{Bmatrix} \mathbf{0} \\ \mathbf{M}^{-1}\boldsymbol{\eta}^u \end{Bmatrix} \mathbf{f}^u + \mathbf{w} = \mathbf{g}\left(\mathbf{X}, \boldsymbol{\theta}_1\left(\boldsymbol{\psi}_{J,l}\right), \boldsymbol{\theta}_2, \mathbf{f}\right) + \boldsymbol{\varphi}^u \mathbf{f}^u + \mathbf{w} \tag{38}$$

$$\begin{aligned} \mathbf{y}_{k+1} &= \begin{bmatrix} \ddot{\mathbf{x}}_{m,k+1} \\ \mathbf{x}_{m,k+1} \end{bmatrix} = \begin{bmatrix} \mathbf{L}_a & \mathbf{0} \\ \mathbf{0} & \mathbf{L}_d \end{bmatrix} \begin{bmatrix} \mathbf{M}^{-1}\left[\boldsymbol{\eta}\mathbf{f}_{k+1} - \mathbf{R}\left(\boldsymbol{\theta}_1\left(\boldsymbol{\psi}_{J,l}\right), \boldsymbol{\theta}_2, \mathbf{x}_{k+1}, \dot{\mathbf{x}}_{k+1}\right)\right] \\ \dot{\mathbf{x}}_{k+1} \end{bmatrix} \\ &\quad + \begin{bmatrix} \mathbf{L}_a \mathbf{M}^{-1} \boldsymbol{\eta}^u \mathbf{f}^u_{k+1} \\ \mathbf{0} \end{bmatrix} + \mathbf{v}_{k+1} \\ &= \mathbf{h}\left(\mathbf{X}_{k+1}, \boldsymbol{\theta}_1\left(\boldsymbol{\psi}_{J,l}\right), \boldsymbol{\theta}_2, \mathbf{f}_{k+1}\right) + \boldsymbol{\lambda}^u \mathbf{f}^u_{k+1} + \mathbf{v}_{k+1} \end{aligned} \tag{39}$$

The predicted state vector $\tilde{\mathbf{X}}_{k+1|k}$ is given as

$$\begin{aligned} \boldsymbol{\chi}_{i,k+1|k} &= \boldsymbol{\chi}_{i,k|k} + \int_{k\Delta t}^{(k+1)\Delta t} \mathbf{g}\left(\boldsymbol{\chi}_{i,t|k}, \boldsymbol{\theta}_1\left(\boldsymbol{\psi}_{J,l}\right), \boldsymbol{\theta}_2, \mathbf{f}\right) \mathrm{d}t \\ &\quad + \boldsymbol{\varphi}^u \hat{\mathbf{f}}^u_{k|k} \Delta t; \ \tilde{\mathbf{X}}_{k+1|k} \\ &= \sum_{i=0}^{2N} W_i^m \boldsymbol{\chi}_{i,k+1|k} \end{aligned} \tag{40}$$

The estimated measurement vector $\hat{\mathbf{y}}_{k+1|k+1}$ is rewritten as

$$\hat{\mathbf{y}}_{k+1|k+1} = \sum_{i=0}^{2N} W_i^m \left[\mathbf{h}\left(\boldsymbol{\chi}_{i,k+1|k}, \boldsymbol{\theta}_1\left(\boldsymbol{\psi}_{J,l}\right), \boldsymbol{\theta}_2, \mathbf{f}_{k+1}\right)\right] + \boldsymbol{\lambda}^u \hat{\mathbf{f}}^u_{k+1|k+1} \tag{41}$$

The related error covariance matrices are shown in Eqs. (19), (21) and (22), respectively.

Under the condition that the number of measurements is larger than that of the unknown excitations, $\hat{\mathbf{f}}^u_{k+1|k+1}$ can be computed by minimizing the error Δ_{k+1}

$$\Delta_{k+1} = \mathbf{y}_{k+1} - \mathbf{h}\left(\hat{\mathbf{X}}_{k+1|k+1}, \boldsymbol{\theta}_1\left(\boldsymbol{\psi}_{J,l}\right), \boldsymbol{\theta}_2, \mathbf{f}_{k+1}\right) - \boldsymbol{\lambda}^u \hat{\mathbf{f}}^u_{k+1|k+1} \tag{42}$$

Then, the estimated measurement vector $\hat{\mathbf{y}}_{k+1|k+1}$ is obtained by Eq. (34), and the structural state vector $\hat{\mathbf{X}}_{k+1|k+1}$ and error covariance matrix $\hat{\mathbf{P}}_{\mathbf{X},k+1|k+1}$ are updated by Eqs. (11) and (12), respectively.

In conclusion, the estimated state vector $\hat{\mathbf{X}}$ and estimated excitation vector $\hat{\mathbf{f}}^u$ are implicit functions of scale coefficient vector $\boldsymbol{\psi}_{J,l}$ and time-invariant physical parameter vector $\boldsymbol{\theta}_2$, namely:

$$\hat{\mathbf{X}} = \hat{\mathbf{X}}\left(\boldsymbol{\psi}_{J,l}, \boldsymbol{\theta}_2\right), \ \hat{\mathbf{f}}^u = \hat{\mathbf{f}}^u\left(\boldsymbol{\psi}_{J,l}, \boldsymbol{\theta}_2\right) \tag{43}$$

Similarly, the estimated acceleration is rewritten as

$$\hat{\dot{\mathbf{x}}}\left(\boldsymbol{\psi}_{J,l}, \boldsymbol{\theta}_2\right) = \mathbf{M}^{-1}\Big(\boldsymbol{\eta}\mathbf{f} + \boldsymbol{\eta}^u \hat{\mathbf{f}}^u\left(\boldsymbol{\psi}_{J,l}, \boldsymbol{\theta}_2\right) - \mathbf{R}\left(\boldsymbol{\theta}_1\left(\boldsymbol{\psi}_{J,l}\right), \boldsymbol{\theta}_2, \hat{\mathbf{X}}\left(\boldsymbol{\psi}_{J,l}, \boldsymbol{\theta}_2\right)\right)\Big) \tag{44}$$

Finally, the optimal scale coefficient vector $\widehat{\boldsymbol{\psi}}_{J,l}$ and optimal time-invariant physical parameter vector $\widehat{\boldsymbol{\theta}}_2$ are obtained by minimizing the same objective error function in Eq. (26), and the optimal time-varying physical parameter vector $\widehat{\boldsymbol{\theta}}_1$ is reconstructed by the inverse WMA in Eq. (14).

3.2 Numerical verification: identification of a time-varying nonlinear one-span truss subjected to an unknown force excitation

As shown in Fig. 10, a one-span truss subjected to an unknown white noise excitation is investigated as a more complex numerical example. It is aimed at identifying the stiffness parameter of each member and the Bouc–Wen model parameters with partial acceleration and displacement measurements.

The truss consists of 15 members and 14 DOFs in total, as shown in Fig. 10. In this numerical example, structural parameters are selected as: The length and cross section of each bar is $l_i = 1$ m and $A_i = 7.85 \times 10^{-5}$ m^2 $(i = 1, 2\ldots, 15)$, respectively. The total mass of each bar is constant as $m_i = 54.95$ kg $(i = 1, 2\ldots, 15)$. The Rayleigh damping is adopted with the first two damping ratios assumed as 0.02. The first five-order natural frequencies of the time-invariant truss are 1.46 Hz, 2.99 Hz, 3.92 Hz, 6.32 Hz and 7.31 Hz, respectively. An unknown white noise excitation f^u is applied on the 4th DOF of the truss. The sampling frequency is 50 Hz during the process of dynamic response calculation and the sampling period is 10 s. Six accelerations of the 2nd, 4th, 6th, 8th, 10th and 12th DOFs and two displacements of the 6th and 14th DOFs are polluted with 2% RMS noise and used as measured responses for identification analysis.

Nonlinear damage is assumed in the 2nd bar element with the Bouc–Wen model governed by Eq. (28). The time-varying physical parameters are defined as

$$k_2 = \begin{cases} 1.57 \times 10^5 \text{ N/m}, & 0\text{s} \le t < 5.2\text{s} \\ 1.256 \times 10^5 \text{ N/m}, & 5.2\text{s} \le t \le 10\text{s} \end{cases}$$

$$k_i = 1.57 \times 10^5 \text{ N/m}, \quad 0\text{s} \le t \le 10\text{s} \quad (i = 1, 3, 4, \ldots, 15)$$

$$\beta_2 = \begin{cases} 8000, & 0\text{s} \le t < 5.2\text{s} \\ 10,400, & 5.2\text{s} \le t \le 10\text{s} \end{cases}$$

$$\gamma_2 = \begin{cases} 6000, & 0\text{s} \le t < 5.2\text{s} \\ 8400, & 5.2\text{s} \le t \le 10\text{s} \end{cases}$$

The identified stiffness results using the FUKF-UI method are shown in Fig. 11. k_2 and nonlinear model parameters are expanded by the Db1 wavelet function and the scale level is $J = 7$ based on the studies in Ref.

Fig. 11 Identification results of the truss model using the FUKF-UI method. **a** k_1; **b** k_2; **c** k_3; **d** k_4; **e** k_5; **f** k_6; **g** k_7; **h** k_8; **i** k_9; **j** k_{10}; **k** k_{11}; **l** k_{12}; **m** k_{13}; **n** k_{14}; **o** k_{15}

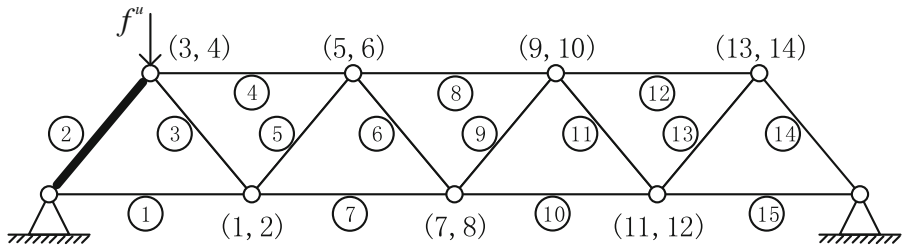

Fig. 10 A one-span truss subjected to an unknown white noise excitation

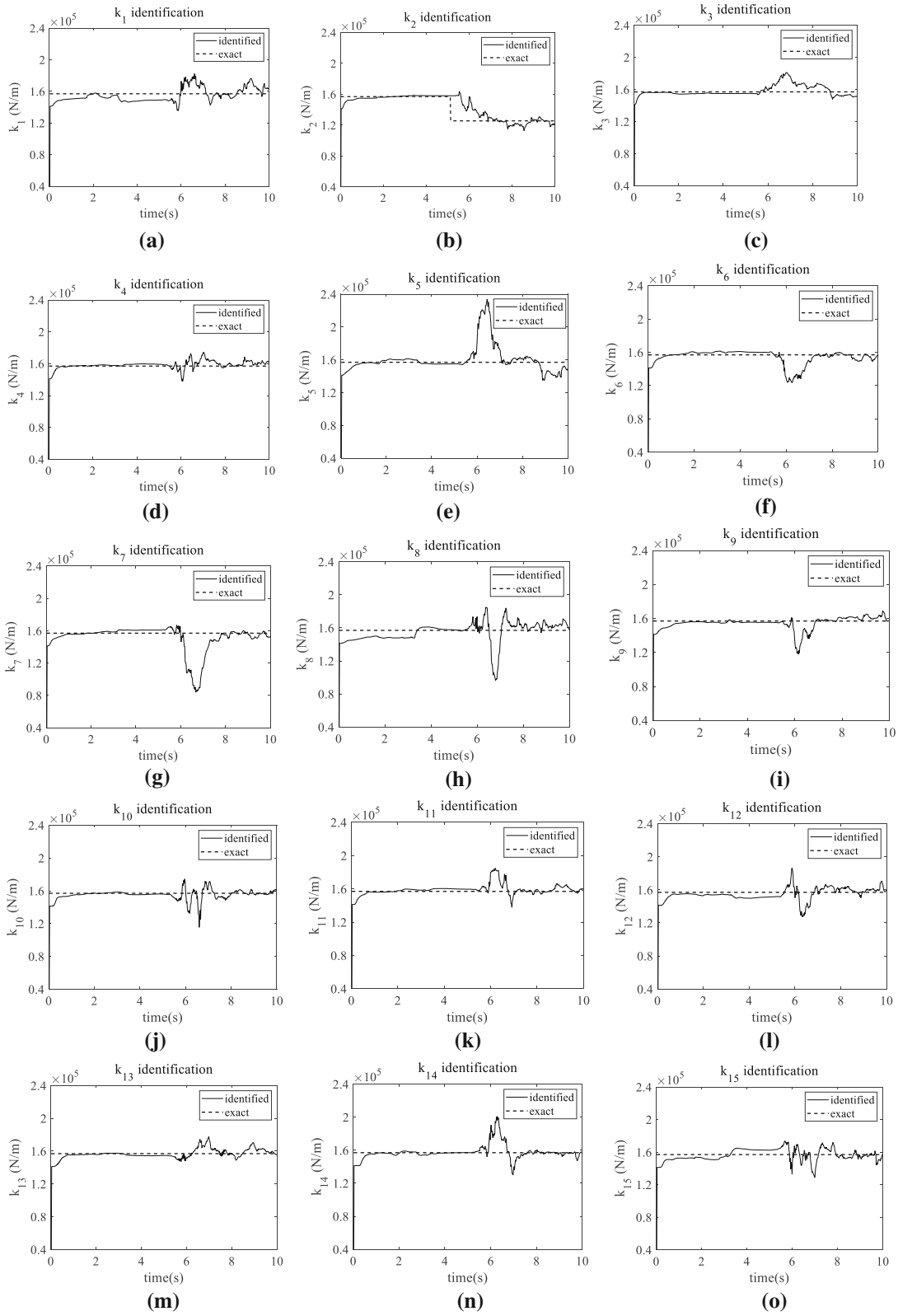
k1 identification
k2 identification
k3 identification
k4 identification
k5 identification
k6 identification
k7 identification
k8 identification
k9 identification
k10 identification
k11 identification
k12 identification
k13 identification
k14 identification
k15 identification
identified
exact
time(s)
(a)
(b)
(c)
(d)
(e)
(f)
(g)
(h)
(i)
(j)
(k)
(l)
(m)
(n)
(o)

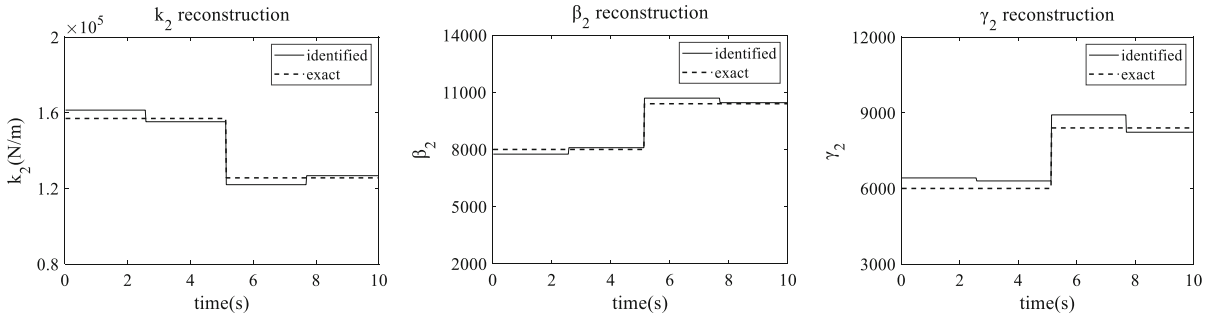

Fig. 12 Comparison of the exact and identified time-varying physical parameters of the truss. **a** k_2; **b** β_2; **c** γ_2

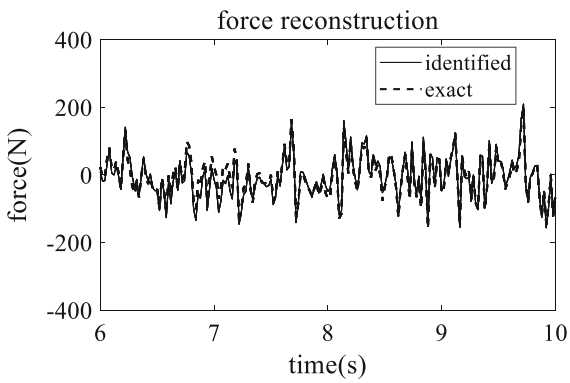

Fig. 13 Comparison of the exact and identified external excitation (6–10 s)

[27]. Figure 12 shows the identified time-varying stiffness parameter and Bouc–Wen model parameters using the proposed WMA integrated with UKF-UI method, which manifests its effectiveness in identifying physical parameters of time-varying nonlinear truss structure with limited number of response measurements and unknown excitations. Meanwhile, the proposed method also gives accurate reconstruction of external force as demonstrated in Fig. 13. Table 1 lists the calculated relative errors of time-invariant stiffness parameters. Most of the relative errors are around 1%, and the maximum value is only 5.29% for the eighth element stiffness parameter.

4 Identification of time-varying nonlinear structures with more number of elements under unknown excitations

It should be noted that the cases discussed above are all about the identification of time-varying nonlinear structures with a small number of elements. With the increasing number of elements, the number of expanded scale coefficients is also significantly increased. Since the basis of the proposed methods in Sect. 2.1.2 and Sect. 3.1.2 is a nonlinear least-squares optimization, a large number of scale coefficients may result in convergence to the local optimization results, especially when the quality of the collected data is poor. Herein, combining the substructural method, a two-step identification process is proposed for the identification of time-varying nonlinear structures with more number of elements under unknown excitations.

4.1 The proposed two-step identification process

4.1.1 Locate the time-varying physical parameters of the whole structure by the proposed FUKF-UI method

The FUKF-UI method proposed in Sect. 3.1.1 is used here to locate the time-varying physical parameters of the whole structure.

Table 1 Identified stiffness of time-invariant members in the truss

Member No.	Actual stiffness (N/m)	Identified stiffness (N/m)	Relative error (%)
1	157,000	159,139.70	1.36
3	157,000	158,973.71	1.26
4	157,000	155,389.34	− 1.03
5	157,000	159,695.78	1.72
6	157,000	162,307.30	3.38
7	157,000	155,094.62	− 1.21
8	157,000	165,298.77	5.29
9	157,000	157,728.76	0.46
10	157,000	156,832.25	− 0.11
11	157,000	156,068.42	− 0.59
12	157,000	159,077.60	1.32
13	157,000	164,468.80	4.76
14	157,000	157,312.26	0.20
15	157,000	159,619.98	1.67

4.1.2 *Divide into substructures and identify the substructural time-varying physical parameters by the proposed WMA integrated with UKF-UI method*

As demonstrated above the proposed WMA integrated with UKF-UI method can accurately identify the actual unknown external loads. Therefore, it can be used to determine the unknown interaction forces acting on the divided substructures in the following substructural-based method.

When aiming at the identification of time-varying nonlinear structures with more elements, the whole structure is divided into several substructures to limit the number of parameters in each optimization analysis. For each substructure, the initial time-varying physical parameter vector $\boldsymbol{\theta}_{s1}$ can be reconstructed by the given time-invariant scale coefficient vector $\boldsymbol{\psi}_{J_s,l_s}$ by Eq. (14). Thus, it is converted into the identification of a time-invariant nonlinear system. The equation of motion of the substructure is written as

$$\begin{aligned}&\mathbf{M}_s\ddot{\mathbf{x}}_s+\mathbf{R}_s\left(\boldsymbol{\theta}_{s1}\left(\boldsymbol{\psi}_{J_s,l_s}\right),\boldsymbol{\theta}_{s2},\mathbf{x}_s,\dot{\mathbf{x}}_s\right)=\boldsymbol{\eta}_s\mathbf{f}_s+\boldsymbol{\eta}_s^u\mathbf{f}_s^u\\&\begin{cases}\boldsymbol{\eta}_s^u=\left[\,\boldsymbol{\eta}_{se}^u\quad\boldsymbol{\eta}_{sb}^*\,\right]\\\mathbf{f}_s^u=\left[\,\mathbf{f}_{se}^u\quad\mathbf{f}_{sb}^*\,\right]^T\end{cases}\end{aligned}\tag{45}$$

in which the subscript "s" indicates that these properties are possessed by the substructure. $\mathbf{M}_s$ is the mass matrix of the substructure. $\mathbf{x}_s$, $\dot{\mathbf{x}}_s$ and $\ddot{\mathbf{x}}_s$ are displacement, velocity and acceleration response vector of substructure, respectively. $\boldsymbol{\theta}_{s2}$ is the time-invariant physical parameter vector of the substructure, $\mathbf{f}_s$ is the known excitation (if have) of the substructure with the influence matrix $\boldsymbol{\eta}_s$ and $\mathbf{f}_s^u$ is the unknown input of the substructure with the influence matrix $\boldsymbol{\eta}_s^u$. $\mathbf{f}_s^u$ is composed of the actual unknown external excitation $\mathbf{f}_{se}^u$ and the unknown substructural interaction force $\mathbf{f}_{sb}^*$, $\boldsymbol{\eta}_{se}^u$ and $\boldsymbol{\eta}_{sb}^*$ are their influence matrix, respectively.

The state space equation and measurement equation are given as

$$\begin{aligned}\dot{\mathbf{X}}_s&=\begin{Bmatrix}\dot{\mathbf{x}}_s\\\ddot{\mathbf{x}}_s\end{Bmatrix}=\begin{Bmatrix}\dot{\mathbf{x}}_s\\\mathbf{M}_s^{-1}\left[\boldsymbol{\eta}_s\mathbf{f}_s-\mathbf{R}_s\left(\boldsymbol{\theta}_{s1}\left(\boldsymbol{\psi}_{J_s,l_s}\right),\boldsymbol{\theta}_{s2},\mathbf{x}_s,\dot{\mathbf{x}}_s\right)\right]\end{Bmatrix}\\&\quad+\begin{Bmatrix}\mathbf{0}\\\mathbf{M}_s^{-1}\boldsymbol{\eta}_s^u\end{Bmatrix}\mathbf{f}_s^u+\mathbf{w}_s\\&=\mathbf{g}_s\left(\mathbf{X}_s,\boldsymbol{\theta}_{s1}\left(\boldsymbol{\psi}_{J_s,l_s}\right),\boldsymbol{\theta}_{s2},\mathbf{f}_s\right)+\boldsymbol{\varphi}_s^u\mathbf{f}_s^u+\mathbf{w}_s\end{aligned}\tag{46}$$

$$\begin{aligned}\mathbf{y}_{s,k+1}&=\begin{bmatrix}\ddot{\mathbf{x}}_{sm,k+1}\\\mathbf{x}_{sm,k+1}\end{bmatrix}=\begin{bmatrix}\mathbf{L}_{sa}&\mathbf{0}\\\mathbf{0}&\mathbf{L}_{sd}\end{bmatrix}\\&\begin{bmatrix}\mathbf{M}_s^{-1}\left[\boldsymbol{\eta}_s\mathbf{f}_{s,k+1}-\mathbf{R}_s\left(\boldsymbol{\theta}_{s1}\left(\boldsymbol{\psi}_{J_s,l_s}\right),\boldsymbol{\theta}_{s2},\mathbf{x}_{s,k+1},\dot{\mathbf{x}}_{s,k+1}\right)\right]\\\dot{\mathbf{x}}_{s,k+1}\end{bmatrix}\\&\quad+\begin{bmatrix}\mathbf{L}_{sa}\mathbf{M}_s^{-1}\boldsymbol{\eta}_s^u\mathbf{f}_{s,k+1}^u\\\mathbf{0}\end{bmatrix}+\mathbf{v}_{s,k+1}\\&=\mathbf{h}_s\left(\mathbf{X}_{s,k+1},\boldsymbol{\theta}_{s1}\left(\boldsymbol{\psi}_{J_s,l_s}\right),\boldsymbol{\theta}_{s2},\mathbf{f}_{s,k+1}\right)+\boldsymbol{\lambda}_s^u\mathbf{f}_{s,k+1}^u+\mathbf{v}_{s,k+1}\end{aligned}\tag{47}$$

where $\mathbf{w}_s$ is the process noise, $\mathbf{y}_{s,k+1}$ is the substructural measurements at the time instant $t = (k+1)\Delta t$ including the partially measured acceleration response $\ddot{\mathbf{x}}_{sm,k+1}$ and displacement response $\mathbf{x}_{sm,k+1}$. $\mathbf{L}_{sa}$ and $\mathbf{L}_{sd}$ are position matrices of accelerometer and displacement responses in the substructure, respectively. $\mathbf{v}_s$ is the measurement noise.

Following the procedure of UKF-UI, the estimated state vector of substructure $\hat{\mathbf{X}}_s$ and unknown excitation vector $\hat{\mathbf{f}}_s^u$ can be obtained, which are implicit functions of scale coefficient vector $\boldsymbol{\psi}_{J_s,l_s}$ and time-invariant physical parameter vector $\boldsymbol{\theta}_{s2}$, that is

$$\hat{\mathbf{X}}_s = \hat{\mathbf{X}}_s\left(\boldsymbol{\psi}_{J_s,l_s}, \boldsymbol{\theta}_{s2}\right),\ \hat{\mathbf{f}}_s^u = \hat{\mathbf{f}}_s^u\left(\boldsymbol{\psi}_{J_s,l_s}, \boldsymbol{\theta}_{s2}\right) \tag{48}$$

Similarly, the estimated acceleration is rewritten as

$$\begin{aligned}\hat{\ddot{\mathbf{x}}}_s\left(\boldsymbol{\psi}_{J_s,l_s}, \boldsymbol{\theta}_{s2}\right) = \mathbf{M}_s^{-1}\Big(&\boldsymbol{\eta}_s\mathbf{f}_s + \boldsymbol{\eta}_s^u\hat{\mathbf{f}}_s^u\left(\boldsymbol{\psi}_{J_s,l_s}, \boldsymbol{\theta}_{s2}\right)\\ &-\mathbf{R}_s\left(\boldsymbol{\theta}_{s1}\left(\boldsymbol{\psi}_{J_s,l_s}\right), \boldsymbol{\theta}_{s2}, \hat{\mathbf{X}}_s\left(\boldsymbol{\psi}_{J_s,l_s}, \boldsymbol{\theta}_{s2}\right)\right)\Big)\end{aligned} \tag{49}$$

Finally, the optimal scale coefficient vector $\widehat{\boldsymbol{\psi}}_{J_s,l_s}$ and optimal time-invariant physical parameter vector $\widehat{\boldsymbol{\theta}}_{s2}$ for the substructure are obtained by minimizing the objective error function in Eq. (50). Then, the optimal time-varying physical parameter vector $\widehat{\boldsymbol{\theta}}_{s1}$ is reconstructed by the inverse WMA.

$$\left[\widehat{\boldsymbol{\psi}}_{J_s,l_s}, \widehat{\boldsymbol{\theta}}_{s2}\right] = \arg\min_{\boldsymbol{\psi}_{J_s,l_s}, \boldsymbol{\theta}_{s2}}\left(\left\|\ddot{\mathbf{x}}_{sm} - \mathbf{L}_{sa}\hat{\ddot{\mathbf{x}}}_s\left(\boldsymbol{\psi}_{J_s,l_s}, \boldsymbol{\theta}_{s2}\right)\right\|_2^2\right) \tag{50}$$

Considering that every substructure is independent of each other, the time-varying physical parameters can be identified by using the proposed WMA integrated with UKF-UI method in parallel, which greatly improves the computational efficiency.

4.2 Numerical verification: identification of a time-varying nonlinear ten-story shear frame with an unknown excitation using the substructural method

In this section, a ten-story shear frame under unknown excitation is used to demonstrate the feasibility of the substructural method for the identification of a time-varying nonlinear structure with more number of elements. The mass of each story is $m_i = 2000\ \text{kg}\ \ (i = 1, 2\ldots, 10)$. The first five-order natural frequencies of the time-invariant system are 0.31 Hz, 0.92 Hz, 1.52 Hz, 2.08 Hz and 2.60 Hz, respectively. It is assumed that the nonlinear damage occurs in the first floor and the Bouc–Wen model governed by Eq. (28) is assumed. $n_1 = 1.8$. A white noise excitation is imposed on the top floor to excite the structure, which is assumed unknown in the identification analysis. The corresponding dynamic responses are computed with a sampling frequency of 50 Hz, and the complete sampling period is 10 s. The specific expressions of other physical parameters are given as

$$k_1 = \begin{cases} 3.0\times10^5\ \text{N/m}, & 0\text{s} \le t < 5.2\text{s} \\ 2.4\times10^5\ \text{N/m}, & 5.2\text{s} \le t \le 10\text{s} \end{cases}$$

$$k_7 = \begin{cases} 3.5\times10^5\ \text{N/m}, & 0\text{s} \le t < 5.2\text{s} \\ 2.73\times10^5\ \text{N/m}, & 5.2\text{s} \le t \le 10\text{s} \end{cases}$$

$$k_{10} = \begin{cases} 3.5\times10^5\ \text{N/m}, & 0\text{s} \le t < 5.2\text{s} \\ 2.975\times10^5\ \text{N/m}, & 5.2\text{s} \le t \le 10\text{s} \end{cases}$$

$$k_i = 3.5\times10^5\ \text{N/m},\ \ 0\text{s} \le t \le 10\text{s}\ \ (i = 2, \cdots, 6, 8, 9)$$

$$c_i = 1000\ \text{N}\cdot\text{s/m},\ \ 0\text{s} \le t \le 10\text{s}\ \ (i = 1, \cdots, 10)$$

$$\beta_1 = \begin{cases} 600, & 0\text{s} \le t < 5.2\text{s} \\ 780, & 5.2\text{s} \le t \le 10\text{s} \end{cases}$$

$$\gamma_1 = 600,\ \ 0\text{s} \le t \le 10\text{s}$$

The FUKF-UI method is implemented to roughly locate the changing physical parameters. Six acceleration measurements at the 1st, 3rd, 5th, 7th, 8th and 10th floors and two interlayer displacements of the 1st–2nd and 9th–10th floors are used. Each response is contaminated with a 2% RMS white noise. The stiffness identification results are shown in Fig. 14. The stiffness of the 1st, 7th and 10th stories is more likely to change, as they transit from one stable convergence value to the other stable value, while other stiffness values are more likely to remain unchanged, since only one convergence value appears despite occasional fluctuations.

The whole structure is divided into two substructures as illustrated in Fig. 15, and the physical parameters in each substructure are identified using the proposed WMA integrated with UKF-UI method in parallel.

Lower substructure

In this numerical example, the 1st–5th DOFs are in the scope of the lower substructure. The accelerations

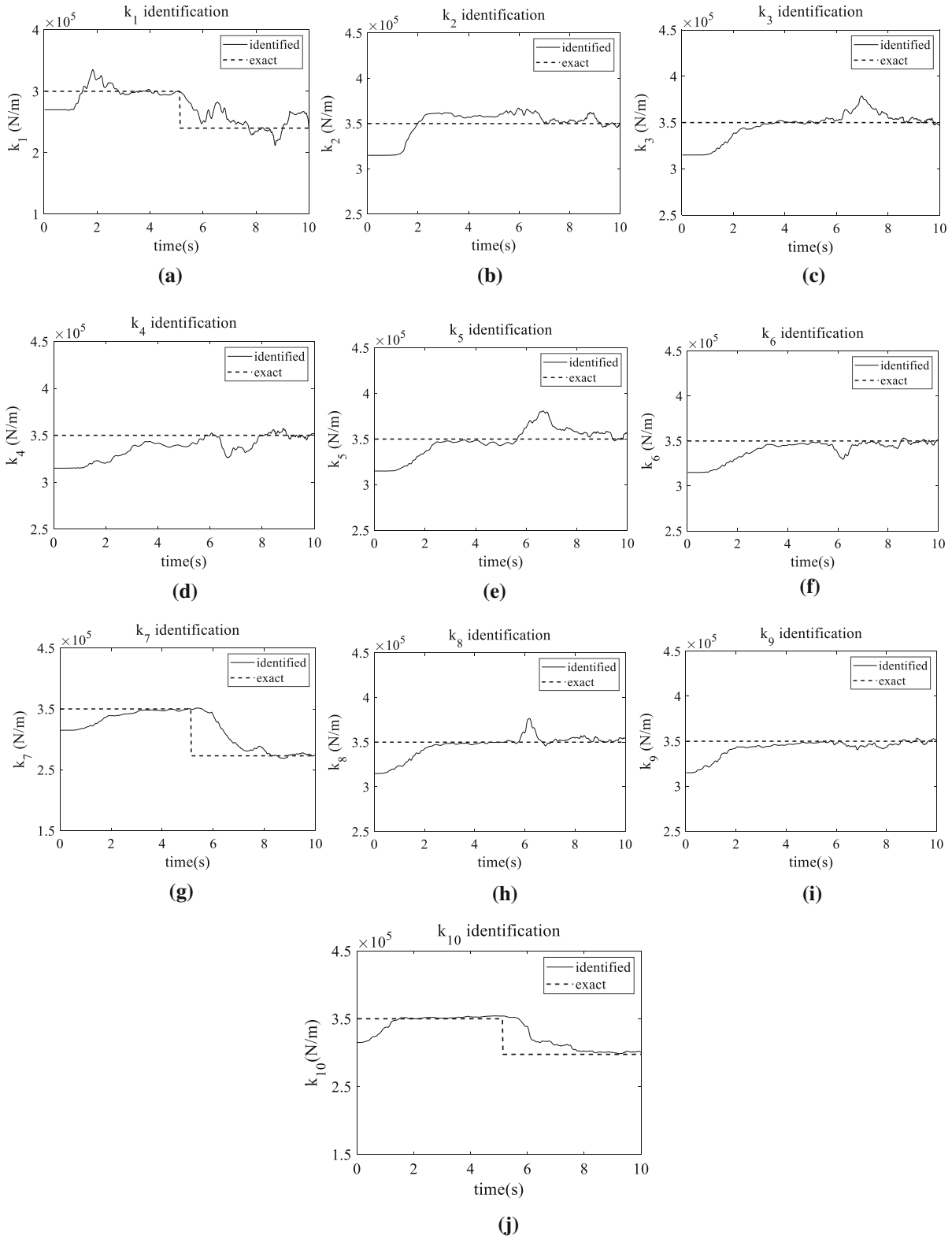

Fig. 14 Identification results using the FUKF-UI method in the shear frame. **a** k_1; **b** k_2; **c** k_3; **d** k_4; **e** k_5; **f** k_6; **g** k_7; **h** k_8; **i** k_9; **j** k_{10}

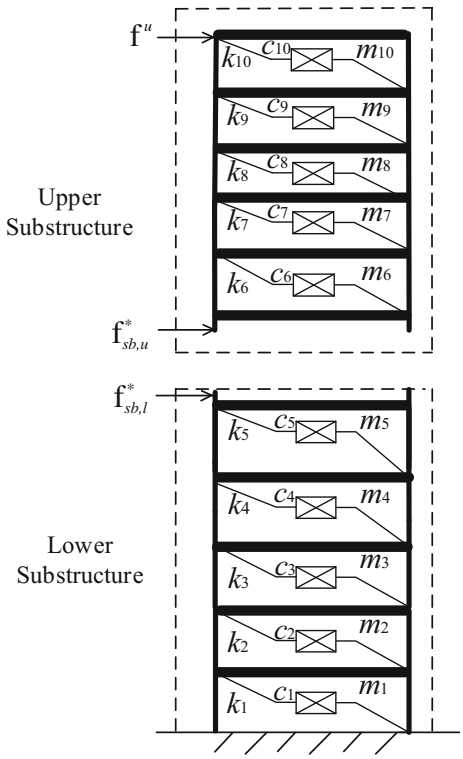

Fig. 15 Substructures of a ten-story shear frame

of the 1st, 3rd and 5th floors and interlayer displacement of the 1st–2nd floors are measured with a 2% RMS noise and used as recorded responses for the identification analysis. k_1, β_1 and γ_1 are expanded by the Db1 wavelet function and the scale level is $J = 7$ [27]. Figure 16 exhibits the identified stiffness and nonlinear model parameters inside the lower substructure employing the WMA integrated with UKF-UI method. The results demonstrate that the identification accuracy is good, even the step changes in time-varying physical parameters can be identified accurately.

Upper substructure

The upper substructure is composed of 6–10 DOFs. The accelerations of the 6th, 8th and 10th floors and interlayer displacement of the 9th–10th floors are used as measurements with a 2% RMS noise for the identification analysis. k_7 and k_{10} are expanded by the Db1 wavelet function and the scale level is $J = 7$. Figure 17 displays the identified stiffness parameters inside the upper substructure, which demonstrates that the proposed WMA integrated with UKF-UI method is capable of the parametric identification of structures with more number of elements when combining with the substructural method. The external load applied on the top floor can also be identified as shown in Fig. 18, which shows that the identified force matches well with the exact one.

5 Conclusions

The identification of time-varying nonlinear structural physical parameters is an important research topic with practical applications. Methods based on WMA can not only identify the time-varying physical parameters such as stiffness and damping coefficients but also the time-varying parameters in the nonlinear model. However, they require displacement, velocity and acceleration responses of all DOFs, and known excitations to be used in the analysis. Moreover, all physical parameters are expanded into scale coefficients by WMA, which leads to a large number of scale coefficients and increases the difficulties in nonlinear system identification. This paper presents two-step identification processes using partial measurements to identify the time-varying physical parameters of nonlinear systems.

Firstly, the identification of time-varying nonlinear structures with a small number of elements under known excitations is conducted. The time-varying physical parameters are distinguished using the FUKF method. Then, a method integrating WMA and UKF is proposed to identify the physical parameters in the case of known excitations. The proposed identification process contributes to reduce the number of scale coefficients, since not all physical parameters are required to be expanded after the locations of time-varying physical parameters are detected. Most importantly, only partial response measurements are needed in the identification process, a clear improvement in the previous WMA-based methods which require response measurements at all DOFs.

Secondly, it is extended to the identification of time-varying nonlinear structures with a small number of elements but under unknown excitations. The time-varying physical parameters are localized using the proposed FUKF-UI method, and then, all the physical parameters, as well as the excitations, are identified by the proposed WMA integrated with UKF-UI method. The proposed identification process meets the needs of practical engineering applications, since the physical

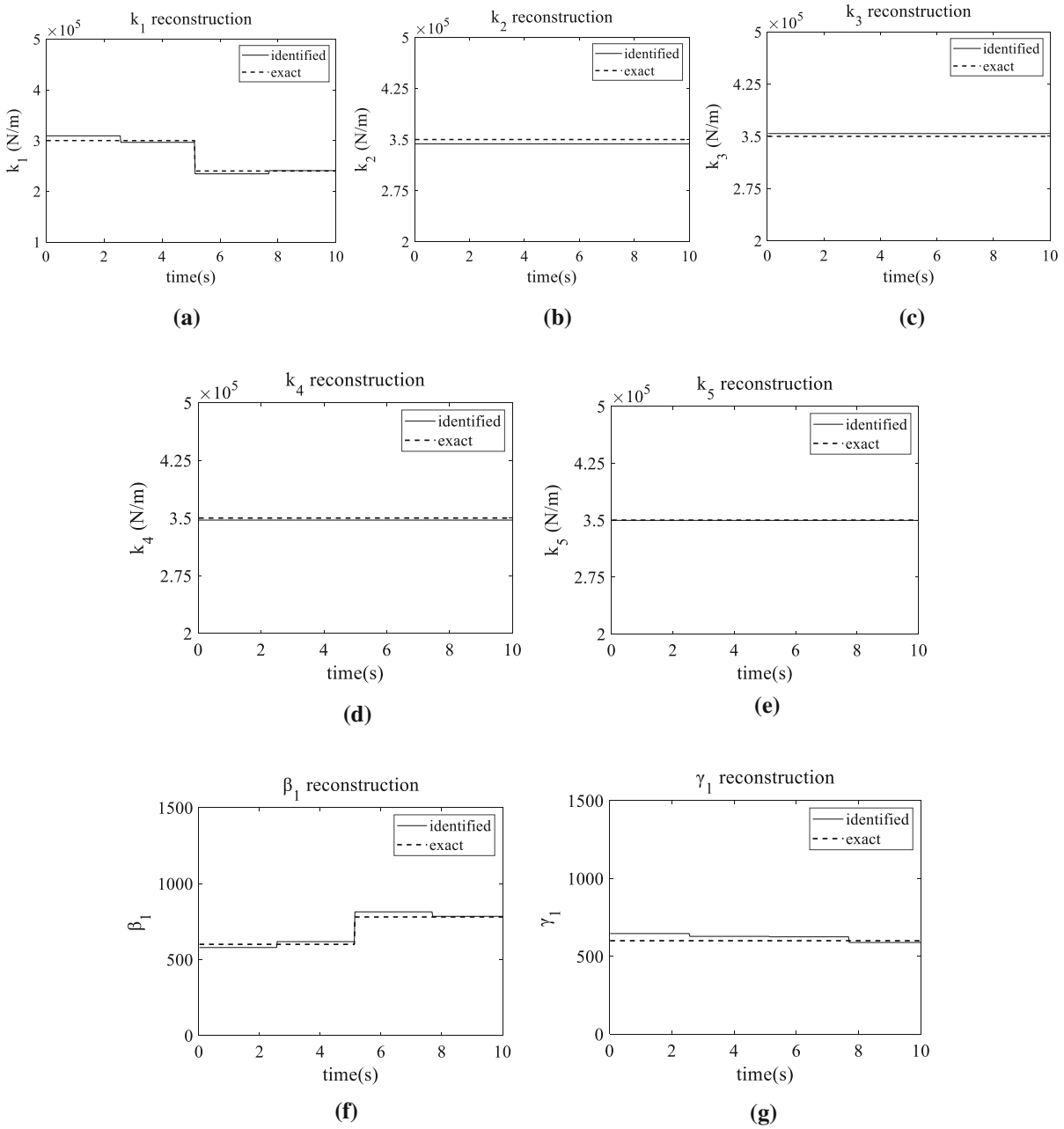

Fig. 16 Comparison of the exact and identified physical parameters of the lower substructure. **a** k_1; **b** k_2; **c** k_3; **d** k_4; **e** k_5; **f** β_1; **g** γ_1

parameters of time-varying nonlinear system can be identified by using partial response measurements under unknown excitations.

Thirdly, combining with the substructural method, it is further extended to identify the time-varying nonlinear structures with more number of elements under unknown excitations. The time-varying physical parameters of the whole structure are located by the proposed FUKF-UI method. Then, the whole structure is divided into several substructures. Based on the proposed WMA integrated with UKF-UI method, each substructure is identified by considering

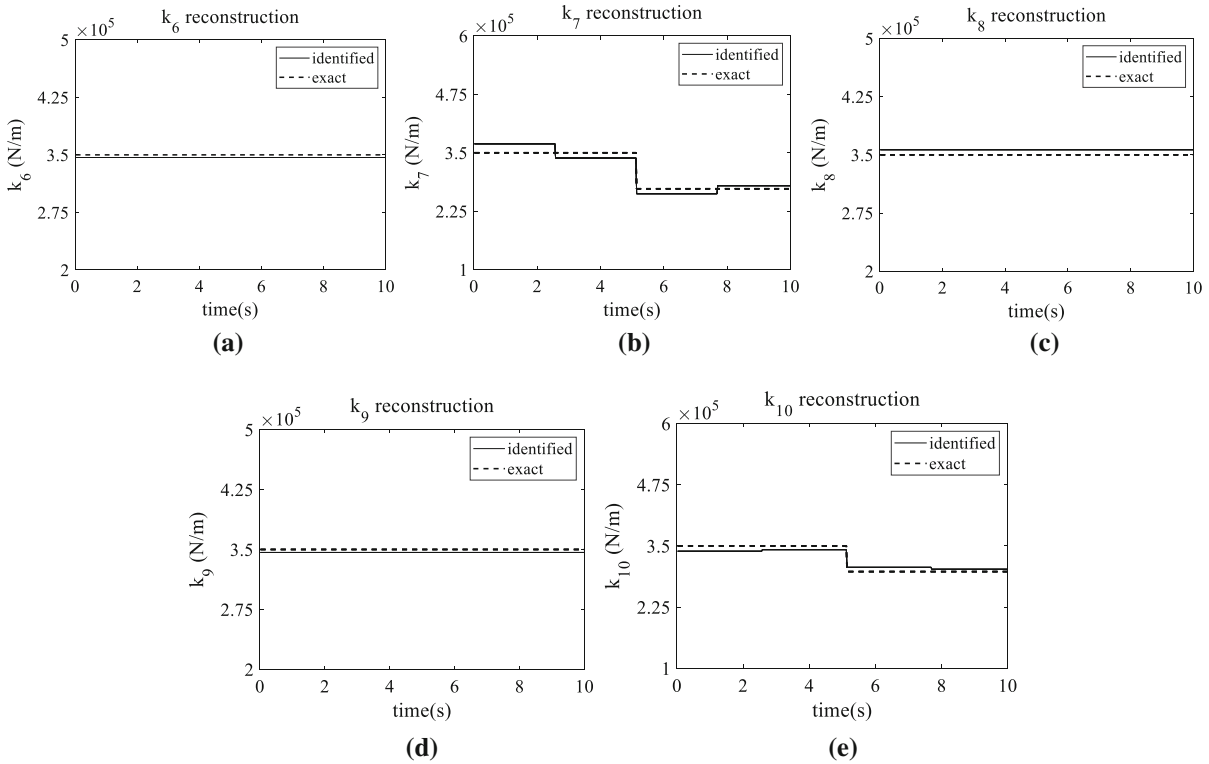

Fig. 17 Comparison of the exact and identified physical parameters of the upper substructure. **a** k_6; **b** k_7; **c** k_8; **d** k_9; **e** k_{10}

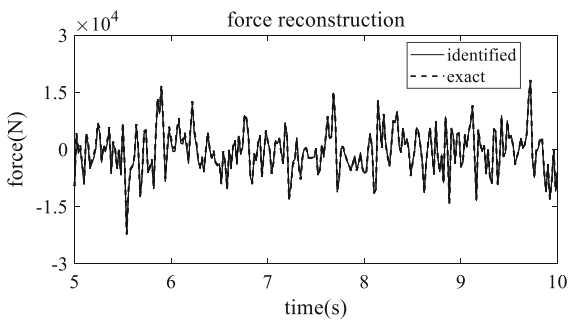

Fig. 18 Comparison of the exact and identified external excitations (5–10 s)

the unknown interaction forces as the fictitious unknown inputs. With partial response measurements, each substructure can be identified in parallel without measuring the interaction forces.

Three numerical examples with noisy measurement data are conducted to verify the effectiveness and accuracy of the proposed identification methods. Experimental verification is still required in future to further demonstrate the efficiency of the proposed methods.

Acknowledgements This research is supported by the National Natural Science Foundation of China through the key project No. 51838006.

Declarations

Conflict of interest The authors declare that they have no conflict of interest concerning the publication of this manuscript.

References

1. Xin, Y., Hao, H., Li, J.: Time-varying system identification by enhanced empirical wavelet transform based on synchroextracting transform. Eng. Struct. **196**, 109313 (2019)
2. Li, J.T., Zhu, X.Q., Law, S.S., Samali, B.: Time-varying characteristics of bridges under the passage of vehicles using synchroextracting transform. Mech. Syst. Signal Process. **140**, 106727.1-106727.19 (2020)
3. Bao, Y.Q., Chen, Z.C., Wei, S.Y., Xu, Y., Tang, Z.Y., Li, H.: Thestate of the art ofdata science andengineering instructural healthmonitoring.Engineering **5**(2),234–242 (2019)
4. Bao,Y.Q., Li, H.: Machine learningparadigm forstructural health monitoring. Struct. Health Monitor. **20**(4), 1353–1372 (2020)
5. Huang, Q., Xu, Y.L., Liu, H.J.: An efficient algorithm for simultaneous identification of time-varying structural

parameters and unknown excitations of a building structure. Eng. Struct. **98**, 29–37 (2015)
6. Yang, J.N., Lin, S.L.: On-line identification of non-linear hysteretic structures using an adaptive tracking technique. Int. J. Non Linear Mech. **39**(9), 1481–1491 (2004)
7. Mu, H.Q., Kuok, S.C., Yuen, K.V.: Stable robust extended Kalman filter. J. Aerosp. Eng. B **30**, 4016010 (2016)
8. Wang, C., Ren, W.X., Wang, Z.C., Zhu, H.P.: Time-varying physical parameter identification of shear type structures based on discrete wavelet transform. Smart Struct. Syst. **14**(5), 831–845 (2014)
9. Xiang, M., Xiong, F., Shi, Y.F., Dai, K.S., Ding, Z.B.: Wavelet multi-resolution approximation of time-varying frame structure. Adv. Mech. Eng. **10**(8), 1–19 (2018)
10. Wang, C., Ai, D.M., Ren, W.X.: A wavelet transform and substructure algorithm for tracking the abrupt stiffness degradation of shear structure. Adv. Struct. Eng. **22**(5), 1136–1148 (2019)
11. Chen, S.Y., Lu, J.B., Lei, Y.: Identification of time-varying systems with partial acceleration measurements by synthesis of wavelet decomposition and Kalman filter. Adv. Mech. Eng. **12**(6), 168781402093046 (2020)
12. Lei, Y., Yang, N.: Simultaneous identification of structural time-varying physical parameters and unknown excitations using partial measurements. Eng. Struct. **214**, 110672 (2020)
13. Quaranta, G., Lacarbonara, W., Masri, S.F.: A review on computational intelligence for identification of nonlinear dynamical systems. Nonlinear Dyn. **99**, 1709–1761 (2020)
14. Xu, Y., Wei, S.Y., Bao, Y.Q., Li, H.: Automatic seismic damage identification of reinforced concrete columns from images by a region-based deep convolutional neural network. Struct. Control Health Monit. **26**(3), e2313 (2019)
15. Xu, B., He, J., Dyke, S.J.: Model-free nonlinear restoring force identification for SMA dampers with double Chebyshev polynomials: approach and validation. Nonlinear Dyn. **82**(3), 1–16 (2015)
16. Wei, S., Peng, Z.K., Dong, X.J., Zhang, W.M.: A nonlinear subspace-prediction error method for identification of nonlinear vibrating structures. Nonlinear Dyn. **91**, 1605–1617 (2018)
17. He, J., Xu, B., Masri, S.F.: Restoring force and dynamic loadings identification for a nonlinear chain-like structure with partially unknown excitations. Nonlinear Dyn. **69**(1–2), 231–245 (2012)
18. Lei, Y., Luo, S.J., He, M.Y.: Identification of model-free structural nonlinear restoring forces using partial measurements of structural responses. Adv. Struct. Eng. **20**(1), 69–80 (2016)
19. Xu, B., Li, J., Dyke, S.J., Deng, B.C., He, J.: Nonparametric identification for hysteretic behavior modelled with a power series polynomial using EKF-WGI approach under limited acceleration and unknown mass. Int. J. Non-linear Mech. 103324 (2019)
20. Cheng, C.M., Peng, Z.K., Zhang, W.M., Meng, G.: Volterra-series-based nonlinear system modeling and its engineering applications: a state-of-the-art review. Mech. Syst. Signal Process. **87**, 340–364 (2017)
21. Wang, Z.C., Ren, W.X., Chen, G.D.: Time-frequency analysis and applications in time-varying/nonlinear structural systems: a state-of-the-art review. Adv. Struct. Eng. **21**, 1562–1584 (2018)
22. Qu, H.Y., Li, T.T., Chen, G.D.: Multiple analytical mode decompositions for nonlinear system identification from forced vibration. Eng. Struct. **173**, 979–986 (2018)
23. Li, H., Mao, C.X., Ou, J.P.: Identification of hysteretic dynamic systems by using hybrid extended Kalman filter and wavelet multiresolution analysis with limited observation. J. Eng. Mech. **139**(5), 547–558 (2013)
24. Ghanem, R., Romeo, F.: A wavelet-based approach for model and parameter identification of non-linear systems. Int. J. Non-Linear Mech. **36**(5), 835–859 (2001)
25. Kougioumtzoglou, I.A., Spanos, P.D.: An identification approach for linear and nonlinear time-variant structural systems via harmonic wavelets. Mech. Syst. Signal Process. **37**(1–2), 338–352 (2013)
26. Yang, Y., Peng, Z.K., Dong, X.J., Zhang, W.M., Meng, G.: Nonlinear time-varying vibration system identification using parametric time–frequency transform with spline kernel. Nonlinear Dyn. **85**(3), 1679–1694 (2016)
27. Chang, C.C., Shi, Y.F.: Identification of time-varying hysteretic structures using wavelet multiresolution analysis. Int. J. Non-Linear Mech. **45**(1), 21–34 (2010)
28. Julier, S.J., Uhlmann, J.K., Durrant-Whyte, H.F.: A new approach for filtering nonlinear systems. Proc. Am. Control Conf. **3**, 1628–1632 (1995)
29. Astroza, R., Alessandri, A., Conte, J.P.: Finite element model updating accounting for modeling uncertainty. Mech. Syst. Signal Process. **115**(15), 782–800 (2019)
30. Lei, Y., Xia, D.D., Erazo, K., Nagarajaiah, S.: A novel unscented Kalman filter for recursive state-input-system identification of nonlinear systems. Mech. Syst. Signal Process. **127**(15), 120–135 (2019)
31. Jwo, D.J., Yang, C.F., Chuang, C.H., Lee, T.Y.: Performance enhancement for ultra-tight GPS/INS integration using a fuzzy adaptive strong tracking unscented Kalman filter. Nonlinear Dyn. **73**(1–2), 377–395 (2013)
32. Hu, G.G., Wang, W., Zhong, Y.M., Gao, B.B., Gu, C.F.: A new direct filtering approach to INS/GNSS integration. Aerosp. Sci. Technol. **77**, 755–764 (2018)
33. Bisht, S.S., Singh, M.P.: An adaptive unscented Kalman filter for tracking sudden stiffness changes. Mech. Syst. Signal Process. **49**(1–2), 181–195 (2014)
34. Wang, N., Li, L., Wang, Q.: Adaptive UKF-based parameter estimation for Bouc–Wen model of magnetorheological elastomer materials. J. Aerosp. Eng. **32**(1), 04018130 (2019)
35. Gaviria, C.A., Montejo, L.A.: Monitoring physical and dynamic properties of reinforced concrete structures during seismic excitations. Constr. Build. Mater. **196**, 43–53 (2019)
36. Koh, C.G., See, L.M., Balendra, T.: Estimation of structural parameters in time domain: a substructure approach. Earthq. Eng. Struct. Dynam. **20**(8), 787–801 (1991)
37. Weng, S., Zhu, H.P., Xia, Y., Gao, F.: Substructuring method in structural health monitoring. Struct. Health Monit. Meas. Methods Pract. Appl. (2017)
38. Yuen, K.V., Huang, K.: Real-time substructural identification by boundary force modeling. Struct. Control Health Monit. **25**(5), e2151.1-e2151.18 (2018)

39. Li, J., Hao, H.: Substructure damage identification based on wavelet-domain response reconstruction. Struct. Health Monit. **13**(4), 389–405 (2014)
40. Liu, K., Law, S.S., Zhu, X.Q.: Substructural condition assessment based on force identification and interface force sensitivity. Int. J. Struct. Stab. Dyn. **15**(2), 1450046 (2015)
41. Ni, P.H., Xia, Y., Li, J., Hao, H.: Improved decentralized structural identification with output only measurements. Measurement **122**, 597–610 (2018)
42. Su, T.L., Tang, Z.Y., Peng, L.Y., Bai, Y.T., Kong, J.L.: Model updating for real time dynamic substructures based on UKF algorithm. Earthq. Eng. Eng. Vib. **19**(2), 413–421 (2020)
43. Kumar, R.K., Shankar, K.: Parametric identification of structures with nonlinearities using global and substructure approaches in the time domain. Adv. Struct. Eng. **12**(2), 195–210 (2009)
44. Tao, D.W., Zhang, D.Y., Li, H.: Structural seismic damage detection using fractal dimension of time-frequency feature. Key Eng. Mater. **558**, 554–560 (2013)
45. Lei, Y., He, M.Y., Liu, C., Lin, S.Z.: Identification of tall shear buildings under unknown seismic excitation with limited output measurements. Adv. Struct. Eng. **16**(11), 1839–1850 (2013)
46. Shi, Y.F., Chang, C.C.: Substructural time-varying parameter identification using wavelet multiresolution approximation. J. Eng. Mech. **138**(1), 50–59 (2012)
47. Shi, Y.F., Chang, C.C.: Wavelet-based identification of time-varying shear-beam buildings using incomplete and noisy measurement data. Nonlinear Eng. **2**, 29–37 (2013)